Mechanical properties of bulk metallic glasses and composites

J. Eckert[a,b] and J. Das
IFW Dresden, Institut für Komplexe Materialien, Postfach 270116, D-01171 Dresden, Germany

S. Pauly
IFW Dresden, Institut für Komplexe Materialien, Postfach 270116, D-01171 Dresden, Germany; and FG Physikalische Metallkunde, FB 11 Material- und Geowissenschaften, Technische Universität Darmstadt, D-64287 Darmstadt, Germany

C. Duhamel
FG Physikalische Metallkunde, FB 11 Material- und Geowissenschaften, Technische Universität Darmstadt, D-64287 Darmstadt, Germany; and IFW Dresden, Institut für Komplexe Materialien, Postfach 270116, D-01171 Dresden, Germany

(Received 17 August 2006; accepted 23 October 2006)

The development of bulk metallic glasses and composites for improving the mechanical properties has occurred with the discovery of many ductile metallic glasses and glass matrix composites with second phase dispersions with different length scales. This article reviews the processing, microstructure development, and resulting mechanical properties of Zr-, Ti-, Cu-, Mg-, Fe-, and Ni-based glassy alloys and also considers the superiority of composite materials containing different phases for enhancing the strength, ductility, and toughness, even leading to a "work-hardening-like" behavior. The morphology, shape, and length scale of the second phase dispersions are crucial for the delocalization of shear bands. The article concludes with some comments regarding future directions of the investigations of spatially inhomogeneous metallic glasses.

I. INTRODUCTION

The first amorphous metal was prepared in 1934 using an evaporation method.[1] Later on, the synthesis of amorphous alloys was also reported by electrodeposition in 1950[2–4] and by splat quenching of Au–Si alloys in the 1960s.[5] After that, (bulk) glass formation in Pd-based,[6–8] Al-based,[9] Mg-based,[10] and Zr-based[11,12] alloys was reported. Even though the mechanical strength of metallic glasses was found in the 1970s and 1980s[13–15] to be superior to that of microcrystalline alloys, at this time the small specimen size restricted conventional mechanical characterization. This was realized only after the production of bulk Zr-based metallic glasses (BMGs).[11,12] The major advantage of metallic glasses is their high elastic strain (~2%), which is much higher than that of common crystalline metallic alloys (<1%). In addition, due to the lack of microstructural features such as grains, grain boundaries, and dislocations, the corrosion resistance[13] and mechanical strength of bulk metallic glasses are very high.[14,15] In Vitreloy 1 ($Zr_{41.25}Ti_{13.75}Cu_{12.5}Ni_{10}Be_{22.5}$), for example, the tensile yield strength σ_y is 1.9 GPa and Young's modulus Y is 96 GPa.[16] The fracture toughnesses (K_{IC}) of Zr-based,[17] Cu-based,[18] Ti-based,[19] and Pd-based[20] glasses are higher (45–85 MPa $m^{1/2}$) than that of Fe-based[21] or Mg-based[19] glasses (2–4 MPa $m^{1/2}$). The macroscopic plastic deformability of bulk metallic glasses is very low, and BMGs show near theoretical strength prior to fracture.[22] The limited macroscopic plastic deformability of BMGs is correlated with highly localized deformation processes, such as shear banding, where a high amount of plastic strain is accumulated in a very narrow region exhibiting strain softening/thermal softening.[23] Even though the local plastic strain in a shear band is very high, the overall room-temperature plastic deformability is disappointingly low.[24]

To circumvent the limited ductility of glassy metallic alloys, the concept of developing a heterogeneous microstructure by combining a glassy matrix with second phase particles with a different length scale has recently been used.[25–28] It was observed that composite microstructures containing crystalline phases show better performance under mechanical stress than monolithic

[a]Address all correspondence to this author.
e-mail: j.eckert@ifw-dresden.de
[b]This author was an editor of this focus issue during the review and decision stage. For the *JMR* policy on review and publication of manuscripts authored by editors, please refer to http://www.mrs.org/jmr_policy.
DOI: 10.1557/JMR.2007.0050

glasses.[24] Besides the details of the state-of-the-art of the synthesis of BMG composites and the evolution of the microstructure, the deformation and fracture behavior of BMG composites will be described for a series of Zr-, Ti-, Cu-, Mg-, Fe-, and Ni-based glassy alloys containing multiple phases with different length scales and volume fractions. Of special interest is the interdependence between preparation conditions, alloy and microstructure design by composition variation, and the resulting mechanical properties of the composites. In addition, recent approaches for obtaining "ductile monolithic" BMGs will be also discussed. Finally, perspectives for future developments in the area of spatially inhomogeneous metallic glasses and their mechanical properties will be discussed.

II. PROCESSING AND MICROSTRUCTURES

A. Processing methods

Metallic glasses can be prepared through "solid-state amorphization" via the mechanical alloying/powder metallurgy route[29,30] and by "rapid cooling" from the liquid state through metal mold casting, melt spinning, or atomization.[9,12,31,32] The powders or flakes obtained through atomization or mechanical alloying must be consolidated in a subsequent step by different techniques such as hot pressing or extrusion[30,33,34] to obtain bulk scale samples. In contrast, the solidification route directly produces bulk specimens (>1 mm).[9,11] BMG composites can also be prepared by these procedures, i.e., through (i) mechanical alloying and consolidation,[35] (ii) solidification,[11,12] or (iii) partial devitrification of amorphous precursors by either thermal treatment[36–38] or severe plastic deformation/high pressure torsion.[39,40] The various processing routes and the evolution of BMG composites with different length scales of second phases are schematically described in Fig. 1.

B. Microstructures

According to their processing history, the microstructures of BMG composites can be classified in two groups: ex situ and in situ formed composites. The microstructural features of these composites can exhibit different features and length scales of second-phase constituents, as exemplified in Fig. 1. The ex situ composites are formed in two ways. The first is mechanical alloying of powders or atomization[41,42] containing a glassy phase and reinforcing second-phase particles, for example, by mixing immiscible oxide nanodispersoids like MgO, CeO_2, Cr_2O_3, and Y_2O_3 into a Mg-based glassy matrix[43] or by adding CaO, ZrO, ZrC, W, and Y_2O_3 into a Zr-based glassy matrix.[44,45] The length scale of these particles varies from micrometer to nanometer scale. Detailed descriptions on the processing and mechanical properties of such composites have been elaborately discussed in Ref. 46. The ex situ composites can also be prepared by directly introducing crystalline second phase(s) as reinforcements into the glass-forming melt during processing.[47–54] In this case, the melt infiltration technique has been frequently used.[47–50] These composites consist of either particle[47–50] or fiber reinforcements[50–54] (continuous or discontinuous fibers). In the case of particulate-reinforced BMG composites Ni, carbon short fibers, W, WC, Ta, Nb, Mo, and SiC[47–50] crystalline particulates have been added to the $Zr_{57}Nb_5Al_{10}Cu_{15.4}Ni_{12.6}$ (Vit-106) melt. Careful investigations suggest a reaction between the particulate and the glass-forming melt, which produces a reaction layer around the reinforcements.[47,48] Nevertheless, the mechanical properties of the composites are improved compared to the monolithic glass.[24] Specifically, attempts on reinforcing $Zr_{41.25}Nb_{13.75}Cu_{12.5}Ni_{10}Be_{22.5}$ (Vit-1) with continuous 1080 steel wires and W particles show significantly improved tensile and compressive properties.[52] A steel wire reinforced composite is shown in Fig. 2. Microstructure observation reveals that the wettability of steel/W with Vit-1 is better, and there is only limited

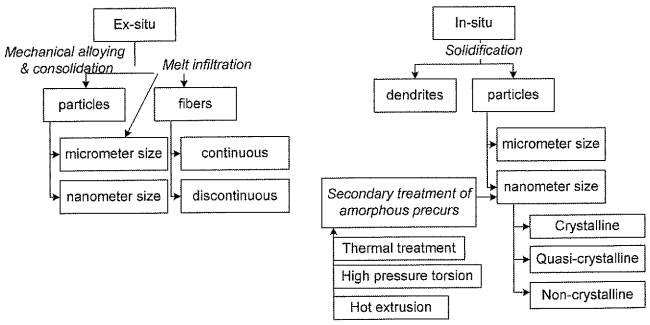

FIG. 1. Different processing routes for obtaining bulk metallic glass matrix composites.

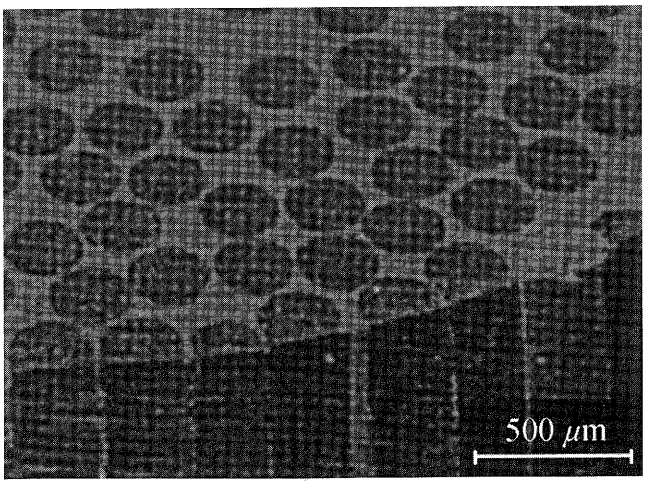

FIG. 2. Ex situ processed steel-wire-reinforced $Zr_{41.25}Nb_{13.75}Cu_{12.5}Ni_{10}Be_{22.5}$ (Vit-1) matrix composite (after Conner et al.[52]).

reactivity at the interface between the fibers and the metallic glass matrix—less than in case of other particulates.[47–50]

The in situ BMG composites are formed either (i) from their melts during appropriate solidification processing or by (ii) a secondary treatment of amorphous precursors. The achievable microstructures with different shape, size, and morphology of second-phase constituents of in situ BMG composites are sketched in Fig. 3. Group (1) of BMG composites requires a sufficient stability of the metastable phases {i.e., nano-micrometer-size quasicrystalline faceted geometry [Fig. 3(a)], nano-micrometer-size crystalline round particle shape [Fig. 3(b)], precipitates with dendritic shape [Fig. 3(c)], or nano-micrometer-size chemically inhomogeneous two phase amorphous phases [Fig. 3(d)]} against the liquid configuration to solidify together with the glassy matrix phase to prepare as-cast BMG composites. Typically, the mechanical properties of in situ composites are superior to those of ex situ composites.[46–53] The preparation of such composites strongly depends on the choice of appropriate alloy compositions and the adopted cooling rates realized during solidification.[55–78] The secondary treatment includes partial devitrification by controlled annealing,[36–38] high-pressure torsion,[39,40] or hot extrusion of amorphous powders.[46]

1. Quasicrystal-BMG composites

Nanometer-sized quasicrystal (QC) reinforced as-spun BMG composites have been prepared in Al–(V,Cr,Mn)–TM,[55] Al–Mn–Ce,[56] and Al–V–Ce–TM[57] (TM = Fe, Co, Ni, Cu) ribbons. For these systems, the formation of quasicrystalline phases together with either an amorphous phase or with an Al-rich matrix strongly depends on the Mn and Ce content in the alloy composition.[56] The QC-Al-based glassy matrix composites are more brittle than QC-reinforced crystalline Al matrix composites.[56] In addition, as-cast micrometer-sized quasicrystal-reinforced BMG composites [Fig. 4(a)] in Zr–Ti–Nb–Cu–Ni–Al[58] and nano-sized QC-BMG composites in $Ti_{40}Zr_{25}Ni_{15-x}Cu_xBe_{20}$ (5 at.% $\leq x \leq$ 15 at.%)[59] have been synthesized in the form of bulk specimens. At higher cooling rates, fully glassy samples can be obtained for these alloys.[58,59] However, the stabilization of a quasicrystalline short-range order strongly depends on the amount of oxygen dissolved in the melt.[60,61] Controlled annealing of $Zr_{65}Al_{7.5}Cu_{17.5-x}Ni_{10}M_x$ (M = Ag, Pd, Au, or Pt; $5 \leq x \leq 10$) at 705–800 K produces nano-quasicrystalline icosahedral (I) phase BMG composites.[62] Some of the nano-QC BMG composites[59,62] show improved room-temperature plastic strain (fracture strain of 5%) compared to monolithic bulk metallic glass.

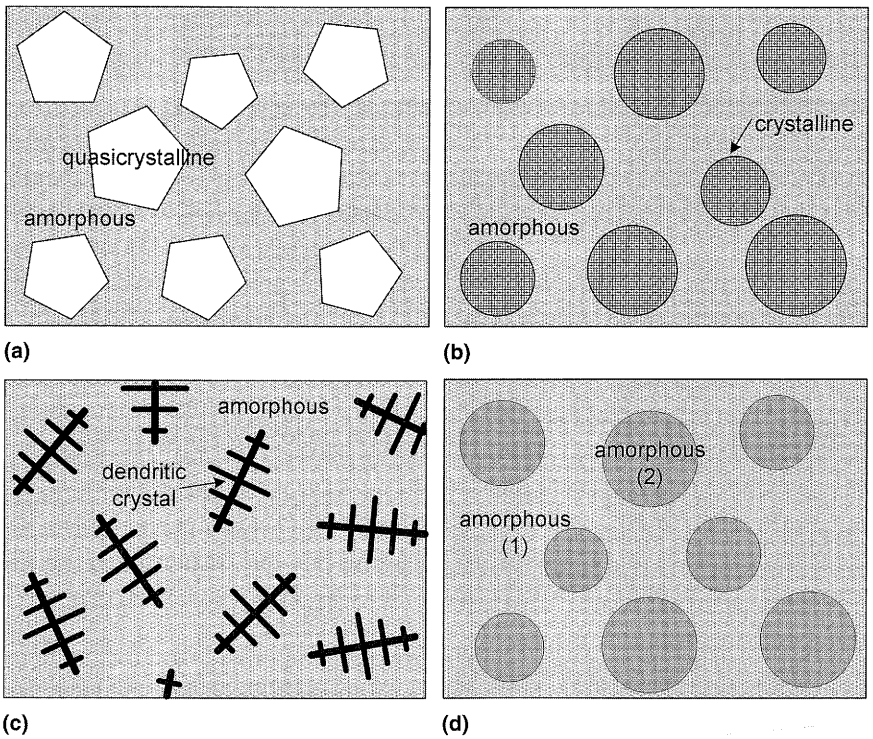

FIG. 3. Schematic representation of microstructures of in situ composites with different second phase dispersions and different length scale with (a) quasicrystalline phase, (b) spherical shaped nano-micrometer-sized crystals, (c) dendritic phase, and (d) two phase amorphous.

2. Crystalline-BMG composites

The preparation of nano-micrometer-size crystalline particle-reinforced BMG composites requires proper design of the alloy composition, an appropriately tuned cooling rate, and/or controlled heat treatment to control the size, morphology, and volume fraction of the second phases. The shape of the crystalline particles is either spherical [Fig. 3(b)] or dendritic [Fig. 3(c)]. For example, in $Zr_{57}Al_{10}Cu_{20}Ni_8Ti_5$, partially devitrified nanocrystalline-BMG composites form after controlled annealing at 673 K. For this alloy, different volume fractions of nanocrystals (40, 45, 68 vol%) have been precipitated by proper annealing treatment.[63] An optimized volume fraction (40 vol%) of nanocrystalline particles has been found for improving the strength. Because crystallization of metallic glasses in Zr-based BMGs often produces Zr_2M-type brittle intermetallic compounds (M = Cu, Ni), the resulting mechanical properties of such nanocomposites are not really superior, but often a tendency for embrittlement that restricts the plastic deformability is observed.[46] However, the size of the primary crystalline phase in $Zr_{57}Al_{10}Cu_{20}Ni_8Ti_5$ is smaller (5–10 nm) than that for $Zr_{55}Cu_{30}Al_{10}Ni_5$ (50–100 nm), which indicates that the presence of the fifth element Ti increases the nucleation rate and decreases the diffusion in the supercooled liquid region, thus limiting the growth rate of the precipitates.[46] This gives some hints for further optimized alloy design and annealing conditions. Recent approaches based on in situ annealing of $Zr_{55}Ti_5Al_{10}Cu_{20}Ni_{10}$, $Zr_{55}Al_{10}Cu_{20}Ni_{10}Pd_5$, and $Zr_{55}Ti_5Al_{7.5}Cu_{22}Ni_8Ga_{2.5}$ in a synchrotron beam show a better control of the size of the nanocrystals (~5 nm) and their homogeneous distribution in the amorphous matrix, as revealed by transmission electron microscopy investigations.[64] Moreover, as-cast bulk nanocrystalline BMG composites (diameter ⩾ 2 mm∅) have been produced in relatively poor glass-forming Cu-based alloys such as $Cu_{60}(Hf/Zr)_{30}Ti_{10}$,[65,66] $Cu_{47}Ti_{33}Zr_{11}Ni_8Si_1$,[67] and $Cu_{60}Zr_{30}Ti_{10}$.[68] A typical microstructure of such as-cast glass matrix nanocrystalline composites is presented in Fig. 4(b). The nanocrystallites correspond to a Cu-rich face-centered cubic (fcc) phase[67] or have a simple cubic structure.[65,66,68]

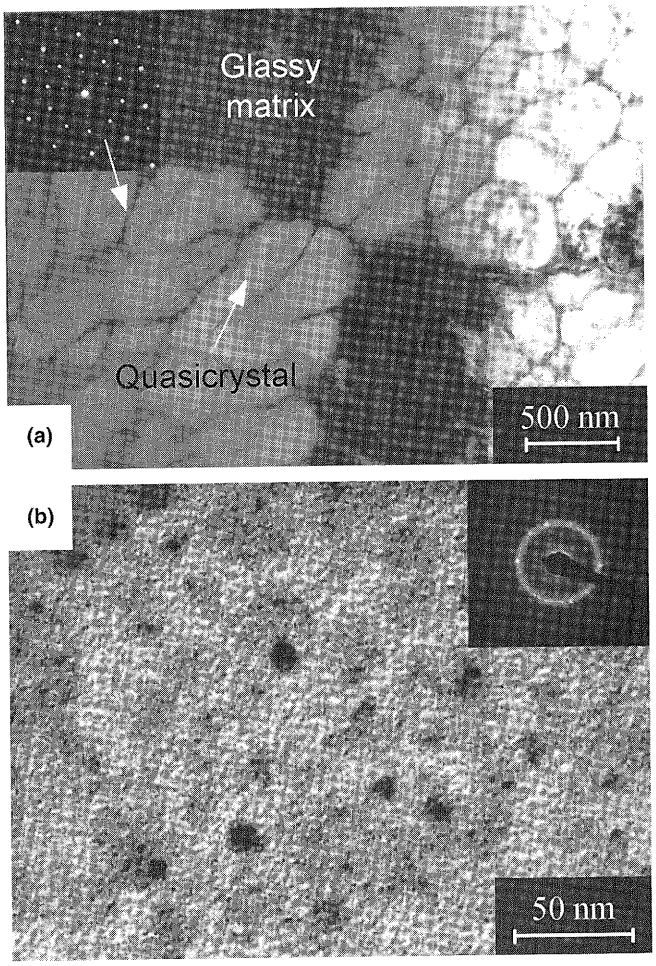

FIG. 4. (a) Micrometer-size quasicrystal reinforced[58] and (b) fcc nanocrystallite reinforced in situ BMG composites.[67]

In recent years, micrometer-sized crystalline particle-reinforced in situ BMG composites have been prepared in several alloy systems. A new era started when Hays et al.[25] reported the preparation of an in situ composite microstructure consisting of ductile body-centered cubic (bcc) β–Zr(Ti) dendrites in a glassy matrix by modifying the Vit-1 composition for a Zr–Ti–Nb–Cu–Ni–Be alloy. This composite exhibits 5–6% compressive plastic strain at room temperature.[25] A similar microstructure [Fig. 5(a)] forms in the case of dendritic bcc β–Zr(Nb) reinforced Zr–Nb–Cu–Ni–Al glassy alloys.[26,27] Moreover, dendritic hexagonal close-packed (hcp) α–Ti reinforced $Ti_{50}Cu_{23}Ni_{20}Sn_7$,[69] Nb-rich dendritic phase reinforced $(Cu_{0.6}Zr_{0.25}Ti_{0.15})_{93}Nb_7$[70] or Ta-rich dendritic phase reinforced $(Cu_{0.50}Hf_{0.35}Ti_{0.10}Ag_{0.05})_{100-x}Ta_x$ ($0 \leqslant x \leqslant 12$ at.%) [Fig. 5(b)] bulk glassy composites[71] have been prepared. In all these cases, the morphology of the second phase is dendritic. The typical design strategy for the preparation of composites is reviewed in Refs. 72 and 73. Based on this idea,[25] a new class of nanocomposite material can be prepared in Ti-based[74–76] and Zr-based[77–79] alloys with bimodal grain size distribution with bcc Ti(Ta/Nb,Sn),[74–76] Zr(Nb),[77,78] or α-hcp Zr (Ni)[79] dendrites embedded in a nanostructured matrix. Along this line, dendritic B2 Ni(Ti,Zr) phase reinforced Ni–(Cu)–Ti–Zr–Si nanocrystalline/BMG composites can be obtained even at very low cooling rates, allowing the preparation of large arc-melted ingots.[80,81] Typically, the casting conditions have a greater impact on the resulting composite microstructure than slight composition variations.[78,82] For example, the dendritic cells in centrifugally cast samples are more spherical with fewer

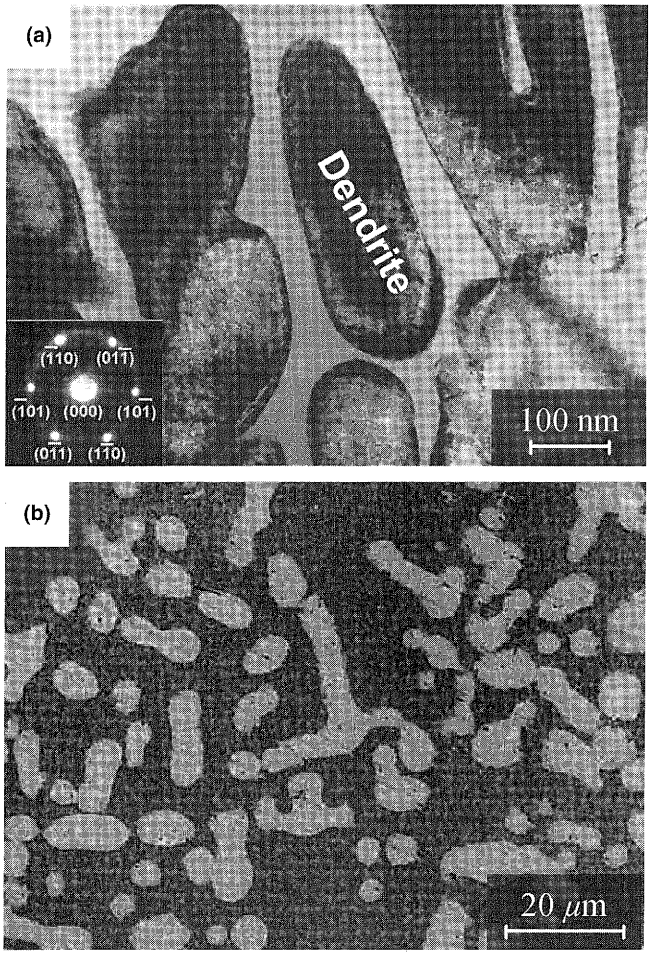

FIG. 5. As-cast (a) bcc β–Zr(Nb) dendritic phase reinforced in situ $Zr_{66.4}Cu_{10.5}Ni_{8.7}Al_8Nb_{6.4}$ composite[26] and (b) Ta-rich dendritic phase reinforced in-situ Cu-based composite.[71]

pronounced secondary arms than in the case of injection or suction cast bulk specimens.[82]

Near spherical particle reinforced in situ BMG matrix composites can be prepared in $(Zr_{0.7}Ni_{0.1}Cu_{0.2})_{82}Al_{10}Ta_8$[83] or $(Cu_{0.6}Zr_{0.3}Ti_{0.1})_{95}Ta_5$[84] alloys by adding Ta to the glass-forming alloy composition. In these cases, 10–20 micrometer-sized Ta(Zr/Ti)-rich[83,84] solid solution phases precipitate during solidification, and the residual melt vitrifies into a high-strength glassy matrix. A similar microstructure forms for body-centered cubic (bcc) α-Fe reinforced $(Mg_{0.65}Cu_{0.075}Ni_{0.075}Zn_{0.05}Ag_{0.05}Y_{0.1})_{100-x}Fe_x$ (x = 9 and 13) BMG composites with high specific strength.[28]

3. Noncrystalline particle-BMG composites–two phase amorphous structures

Phase separation in as-spun metallic glasses was observed long ago in Pd–Au–Si[85] and Pd–Ni–P.[86] Nanometer-scale phase separation also occurs during annealing in the supercooled liquid region in bulk metallic glasses before primary crystallization, for example in Vit-1 ($Zr_{41.25}Nb_{13.75}Cu_{12.5}Ni_{10}Be_{22.5}$).[87] In addition, phase separation in the undercooled melt was also observed in $Mg_{62}Cu_{25}Y_{10}Li_3$ metallic glassy ribbons.[88] Nanoscale "liquid phase" phase separation occurs in $Pd_{40}Ni_{40}P_{20}$,[89] $Pd_{81}Si_{19}$,[90] $Cu_{47.5}Zr_{47.5}Al_5$,[91] $Cu_{47}Ti_{33}Zr_{11}Ni_8Si_1$,[92] $Cu_{43}Zr_{43}Al_7Ag_7$,[93] $Cu_{46}Zr_{47-x}Y_xAl_7$ ($0 \leq x \leq 35$ at.%),[94] $Zr_{28}Y_{28}Al_{22}Co_{22}$,[95] $Ni_{58.5}Nb_{20.25}Y_{21.25}$,[96] $Ni_{60}Nb_{40-x}Sn_x$ ($3 \leq x \leq 9$ at.%),[97] and $Au_{49}Ag_{5.5}Pd_{2.3}Cu_{26.9}Si_{16.3}$[98] bulk metallic glasses in the as-cast state. A typical composite microstructure consisting of two amorphous phases as it develops in Ni–Nb–Y[96] is presented in Fig. 6. The chemical demixing can be explained in terms of a positive enthalpy of mixing[97,98] between the constituent elements or as a preliminary stage of primary crystallization in the supercooled liquid region.[87] Even though two-phase amorphous composites represent a unique structural hierarchy of BMGs, besides the Cu-based alloys,[91,93,94] most of these phase-separated glasses do not show plastic deformability at room temperature, in contrast to what one could expect. This finding is still only poorly understood and certainly requires further investigation.

III. DEFORMATION

The mechanical properties of monolithic BMGs show a unique combination of high strength, from 1 GPa in the case of Mg-based BMGs up to 3–4 GPa in the case of Fe- or Co-based BMGs, and low Young's modulus (80–90 GPa), together with an elastic strain of around 2%.[93] However, the macroscopic ductility of most metallic glasses is rather low.[63] Catastrophic failure occurs soon after yielding, and the plastic deformation is limited to a few percent at best in compression (mostly <1%). To circumvent such limitations and to obtain both high strength and enhanced ductility, a large number of composite microstructures have been recently developed, as

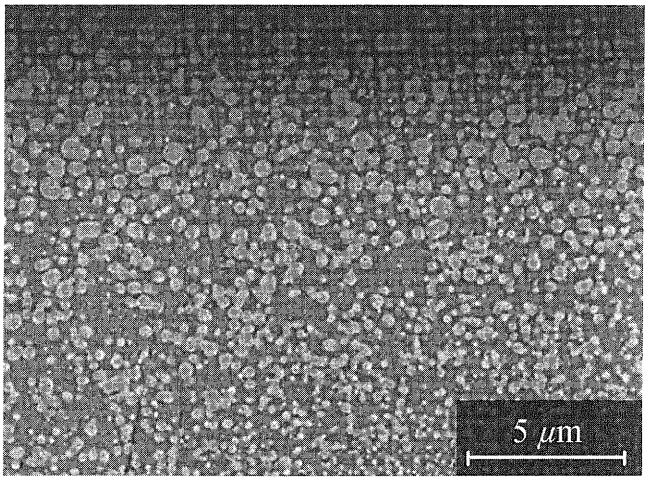

FIG. 6. Two phase amorphous composite in Ni–Nb–Y BMG.[96]

discussed in the former section. The notion of "bulk metallic glass composites" thus refers to a large variety of microstructures and, consequently, to a wide range of mechanical properties. In particular, different combinations of strength and ductility are expected. In the following sections, the influence of the second phase on several issues of mechanical properties of glassy matrix composites will be discussed.

A. Strength and ductility

The factors governing the strength and ductility and the toughening mechanisms in BMG composite microstructures include the properties of the reinforcing phases, such as their elastic properties; their yield strength and ductility for enhancing the load transfer from the matrix to the reinforcing phase(s); and the properties of the interface between the second phase and the glassy matrix in terms of bonding strength and wettability, together with the volume fraction, size, and morphology of the second phases.[99–106]

Usually, the ex situ composites contain a reinforcing phase, such as TiC,[101] TiB_2,[102] WC,[103] ZrC,[104] or ZrO_2[105] particles, W/steel filaments,[52,106] or carbonnanotubes[54] embedded in the glassy matrix, which leads to higher fracture strength with increasing amount of reinforcing phase, as shown in Fig. 7. The strengthening role of the second phase is particularly important for Mg-based BMGs, where, for example, a strength twice as high can be reached by adding 20 vol% TiB_2 particles.[102] However, except for the Zr-based BMGs reinforced with W or steel filaments,[52] the reinforcing effect of the second phase seems to decrease when the volume fraction of the particles becomes too high.[101,107] For example, when 10 vol% WC is added to a Cu–Ti–Zr–Ni–Sn–Si amorphous alloy, the fracture strength increases from 1600 to 2250 MPa. However, further addition of 10 vol% WC only leads to an increase of 150 MPa.[103] In some cases, the fracture strength of the composite even decreases, revealing that the strengthening effect of the second phase changes toward a tendency for embrittlement with increasing volume fraction of particles.[101,107] Generally, the higher fracture strength obtained by the addition of particles or fibers is linked with an improvement of the ductility compared to the monolithic BMG.[24] However, except for the Zr-based BMGs reinforced by W filaments, for which a strain to failure of up to 18.5% has been reported,[52,100] the ductility is still limited to 1–5% plastic deformation. An enhancement of plastic deformation up to 24% has also been reported for a $Zr_{57}Nb_5Al_{10}Cu_{15.4}Ni_{12.6}$ BMG reinforced with Nb particles.[47] In that case, the increase in plastic deformation is mainly due to the ductile nature of the particles and is accompanied by a significant decrease in the flow stress from 1800 to 800 MPa.

Compared to the ex situ process, in situ processing

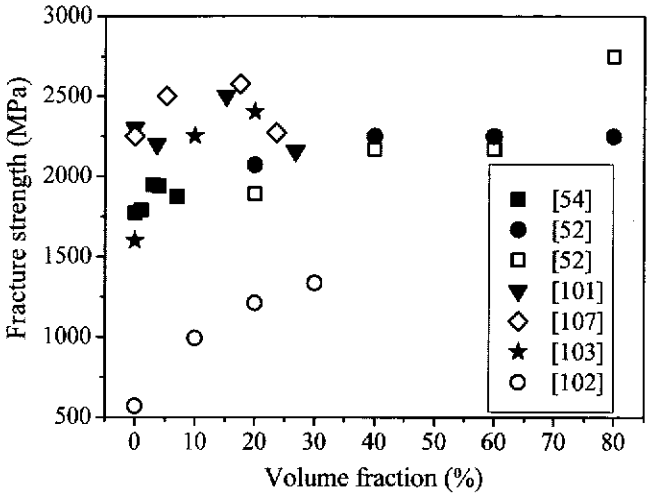

FIG. 7. Compressive fracture strength as a function of the volume fraction of crystalline phase for different ex situ composites. The data are taken from Refs. 52, 54, 101–103, and 107.

usually leads to better bonding between the matrix and the crystalline phase(s).[47–53] The deformation behavior of in situ composites obtained either by partial crystallization of the glass or by precipitation of particles during the casting process strongly depends on two parameters: the volume fraction of the crystallites and their size. The effect of the particle volume fraction on the compressive behavior of the amorphous and partially crystallized $Zr_{57}Cu_{20}Al_{10}Ni_8Ti_5$ alloy is shown in Fig. 8.[63] The partially crystallized samples are obtained by annealing the monolithic BMG and consist of nanoprecipitates with a grain size of 2–10 nm, which are homogeneously distributed in the amorphous matrix. Up to a critical volume fraction of nanocrystals (V_f) of around 40 vol%, the flow stress of the material increases without any detrimental effect on the ductility. For V_f = 45 vol%, the flow stress still increases, but fracture occurs soon after yielding (ϵ_p < 1%). With further increase of V_f, the sample becomes brittle, and a drastic fall of the fracture stress occurs. A similar trend has been observed for Zr–Al–Ni–Cu–Ag[108] and Zr–Ti–Cu–Ni–Al[109] BMGs with nano-quasicrystalline precipitates. The influence of the crystallite size on the mechanical behavior, especially on the ductility, is still unclear. In another case, addition of 1 at.% Si to a Cu–Ti–Zr–Ni BMG leads to a nanophase composite microstructure, which consists of a uniform distribution of fcc nanoscale particles about 8–12 nm in size in an amorphous matrix.[67] On the other hand, addition of 1 at.% Sn instead of Si to the same base composition leads to a microstructure composed of a nonuniform distribution of 10 vol% star-shaped precipitates 3–5 μm in size.[67] While the Cu–Ti–Zr–Ni BMG and the Cu–Ti–Zr–Ni–Sn composite exhibit almost no plastic deformation (ϵ_p < 1%), the Cu–Ti–Zr–Ni–Si alloy is able to sustain up to 2.2% plastic deformation. Bian

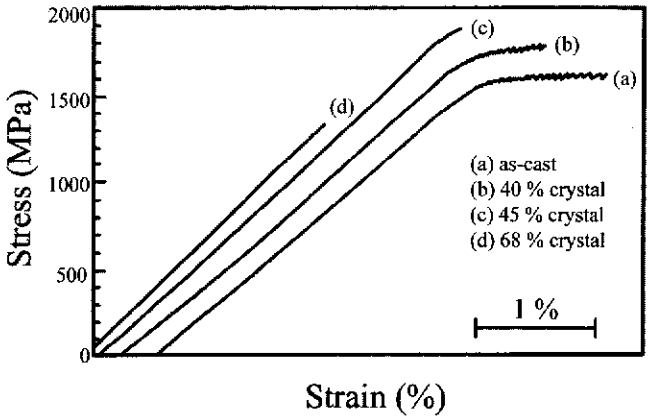

FIG. 8. Compressive stress–strain curves of the amorphous and partially crystallized $Zr_{57}Cu_{20}Al_{10}Ni_8Ti_5$ alloy: (a) as-cast, (b) 40 vol%, (c) 45 vol%, and (d) 68 vol% nanocrystals.[56]

et al. have shown that, by increasing the size of quenched-in crystallites from 300 to 1000 nm, $Zr_{52.5}Cu_{17.9}Ni_{14.6}Al_{10}Ti_5$ composites undergo a ductile-to-brittle transition.[110] Leonhard et al.[63] reported that the formation of 10 vol% micrometer-sized crystallites during casting leads to brittle failure, whereas the same amount of nanocrystals in the glassy matrix does not alter its mechanical properties. On the contrary, in situ $(Zr_{70}–Ni_{10}Cu_{20})_{90-x}Ta_xAl_{10}$ (x = 6, 12) composites containing homogeneously dispersed Ta particles 20–50 μm in size in an amorphous matrix exhibit a large apparent plastic strain in compression (16.6%) as well as work hardening.[111] These composites are obtained by addition of 6–12 at.% Ta to a Zr–Ni–Cu–Al BMG. Apparently, Ta addition has two effects on the resulting microstructure: it leads to the formation of Ta-rich solid solution particles, and it modifies the composition of the glassy matrix, leading to an increase in medium-range order, which carries the plasticity in the amorphous phase.[112] Therefore, the enhanced ductility may result from both contributions of the particles as well as from structural changes in the matrix.

The best combination of high strength and improved ductility is obtained for bulk metallic glass composites containing a ductile dendritic phase.[71] Such composites exhibit enhanced plastic deformation in compression,[25–28,71,113–115] tension,[25,113–115] and bending.[25,116,117] A higher volume fraction of dendrites drastically enhances the ductility in compression (6–20%) with only a limited effect on the yield strength [Figs. 9(a)–9(b)]. Although for Cu-based BMGs a small amount of dendritic phase is sufficient to enhance the plastic deformation considerably,[71] for Zr-based[118] and La-based composites,[114] a critical volume fraction (around 40 vol%) has to be reached for any significant effect on the ductility to be detected. The slight decrease in the yield strength compared to monolithic BMGs is counterbalanced by work hardening, which occurs during plastic deformation of the ductile samples. The resulting fracture strength is, consequently, in the same range[72,114] or even higher than that for the monolithic BMG. The few data available on the tensile behavior of glassy matrix/dendrite composites show that plastic deformation can also be obtained.[115] Fracture occurs after substantial necking, and the local strain can reach 15%.[25,115] Results on La-based[114] and Zr-based[115] composites reveal a stress sensitivity of the yield strength under different testing conditions. For the La-based composites, the compressive yield stresses are 6–31% higher than the values in tension.[114] In crystalline materials, such a yield asymmetry is characteristic for the effect of the normal stress on the slip plane.[119] Donovan was the first to report such a phenomenon for Pd-based metallic glasses.[120] He concluded that yielding of metallic glasses obeys the Mohr–Coulomb yield criterion rather than the von Mises criterion, which is appropriate for polycrystalline metals.[121] The results mentioned

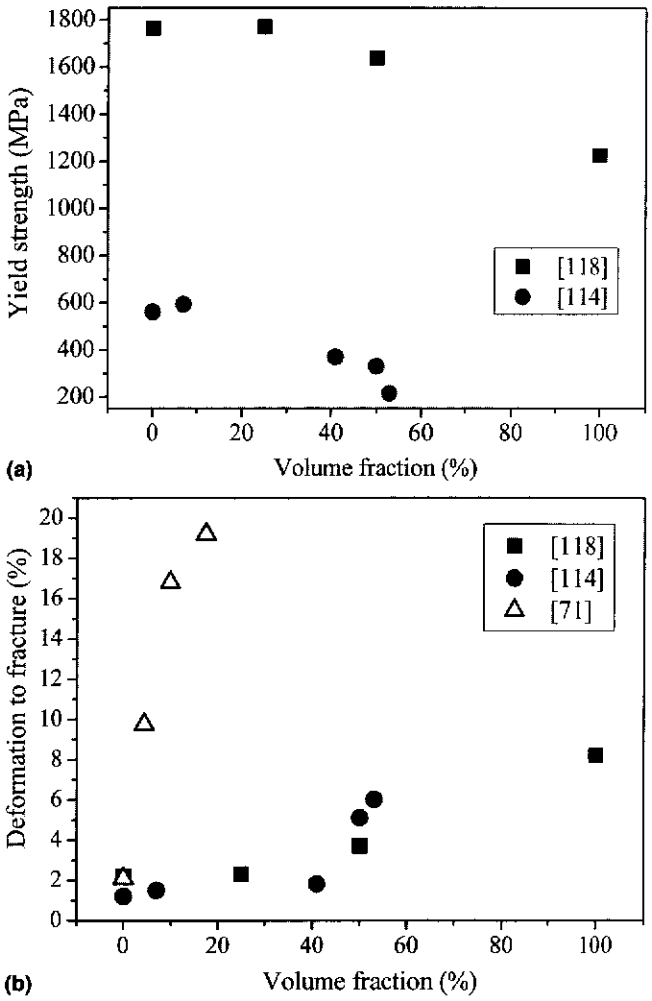

FIG. 9. (a) Compressive yield strength and (b) total strain as a function of the volume fraction of crystalline phase for the glassy matrix/dendrite composites. The data are taken from Refs. 71, 114, and 118.

above for BMG composites are also in agreement with molecular dynamics simulations performed on the deformation of metallic glass, which predict a 24% higher yield stress in compression than in tension.[122] However, the difference between tension and compression decreases with increasing volume fraction of dendrites and, for $V_f = 50\%$, the asymmetry between tension and compression nearly disappears.[114] This may indicate a transition from a glassy phase controlled to a crystalline phase controlled yielding, i.e., from an asymmetric yield criterion (typically of the Mohr–Coulomb type) to a symmetric yield criterion (typically the von Mises criterion). The different yield criteria can be unified in an "ellipse criterion."[123] According to this ellipse criterion, the yielding of materials depends on a material-dependent constant parameter α, which approaches (i) a value $\alpha \rightarrow 0$ for ductile crystalline materials with low strength, (ii) $\alpha \approx 1/3$ to $2/3$ for high-strength materials, such as BMGs or nanostructured materials, and (iii) $\alpha \geq \sqrt{2/2}$ for brittle materials with high hardness, such as rock, intermetallics, ceramics, etc.[123]

B. Hardness

The presence of crystalline second phases in ex situ or in situ composites increases the hardness of the material significantly, as shown in Fig. 10. In most cases, the hardness increases almost linearly with the volume fraction of the crystalline phase, which is consistent with the Tabor relation $H_v = 3\sigma_f$.[121] The strengthening effect of the second phase, already revealed by the increase in the fracture strength, results from the considerable difference in the hardness of the individual phases.[124] For example, the hardness values of the $Cu_{47}Ti_{33}Zr_{11}Ni_6Sn_2Si_1$ matrix and of the TiB reinforcements are 543 and 2500 H_v, respectively.[107] However, the presence of second-phase particles alone is not sufficient to explain the hardness values, especially in the case of the in situ composites where a significant deviation from the rule of mixtures has been reported.[125] For partially devitrified glass, the hardness of the composite is the result of two effects: a phase mixture effect and a change in the composition of the glassy phase. Indeed, in situ crystallization may induce a difference in the composition between the glassy matrix and the precipitates.[126] After partial devitrification, the composition of the remaining glassy matrix is changed compared to that of the starting monolithic glass. Thus, the hardness of the glassy matrix changes with proceeding partial devitrification. Studies of the hardening mechanism of melt-spun Al-based composites have even shown that hardening of the remaining glassy matrix due to solute enrichment during crystallization can be the predominant effect.[127]

A similar effect has been revealed for BMG/dendrite composites.[71] For Cu–Hf–Ti–Ag–Ta composites,[71] the dendrites act as a softening phase, and a decrease of the hardness of the composite is expected with increasing volume fraction of dendrites. However, due to the change in the composition of both the dendrites and the matrix, a decrease of the hardness of the two individual phases is registered when the volume fraction of the dendrites increases. The hardness of the matrix (initially 9.66 GPa for the single phase glass) decreases to 9.63 and 9.36 GPa, and the hardness of the dendrites decreases from 6.0 to 5.21 GPa, when the volume fraction of the dendritic phase increases from 4.3 to 26.5 vol%.

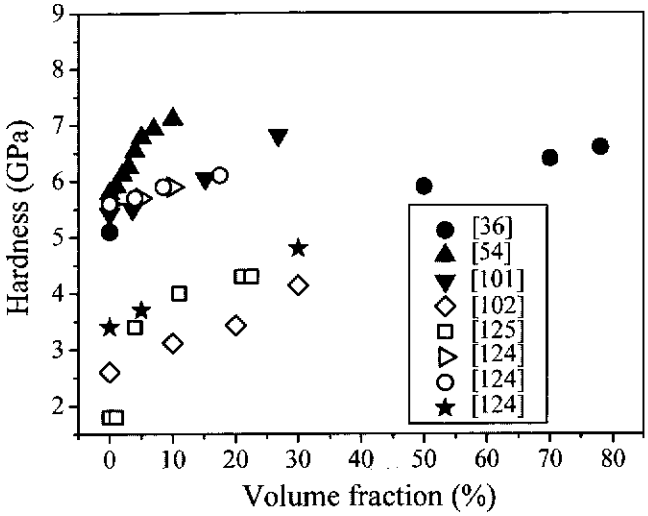

FIG. 10. Hardness as a function of the volume fraction of crystalline phase. The data are taken from Refs. 36, 54, 101, 102, 124, and 125.

C. Fracture energy

In the case of monolithic glasses, the fracture energy, either measured by Charpy impact testing or calculated from the fracture toughness, depends on the composition of the alloy.[17–21] Zr- and Cu-based, as well as some Fe- and Pt-based BMGs exhibit fracture energies between 60 and 90 kJ/m^2 whereas Mg- and Ce-based BMGs and some Fe-base BMGs exhibit values below 10 kJ/m^2. According to Lewandowski et al.,[128] a universal correlation exists between the fracture energy and the elastic modulus ratio μ/B. When the μ/B ratio is low ($\mu/B < 0.41$ to 0.43), the metallic glass is intrinsically ductile, even though it exhibits no macroscopic plastic deformation. Plasticity is then confined to very localized shear bands where the strain can reach up to 100%. On the contrary, for a high μ/B ratio, the material is intrinsically brittle and characteristic cleavage features are observed on the fracture surface. Few studies report the fracture energy of BMG composites, as measured by Charpy impact tests.[114,129] Two different behaviors are observed, depending on the nature of the crystalline phase. Figure 11 shows the fracture energy as a function of the volume fraction of crystals for a La-based glassy matrix-dendrite composite[114] and a partially devitrified La-based

glass.[129] For monolithic $La_{62}Al_{14}(Cu,Ni)_{24}$[114] and $La_{55}Al_{25}Cu_{10}Ni_5Co_5$[129] BMGs, the impact toughness is 17 and 9.43 kJ/m^2, respectively. The data are normalized with respect to the highest measured value.

For the α–La dendritic phase reinforced BMG composites, no significant effect of the crystalline phase on the fracture energy is detected for $V_f < 40\%$.[114] Beyond this value, a drastic increase of the impact toughness is registered, and the fracture energy becomes up to 60% higher (V_f = 50 %) than that for monolithic BMGs. A similar improvement has also been reported for a $Zr_{56.2}Ti_{13.8}Nb_{5.0}Cu_{6.9}Ni_{5.6}Be_{12.5}$ BMG composite[25] where the introduction of 25 vol% β–Zr(Ti,Nb) dendrites increases the toughness from 80 kJ/m^2 for the monolithic BMG to 200 kJ/m^2 for the composite.

However, the glass matrix-nanocrystalline (unknown intermetallics) composite[129] obtained by partial crystallization exhibits the opposite trend (Fig. 11). For $V_f <$ 50%, a drop of the fracture energy by 90% (from 9.43 to 0.79 kJ/m^2) is registered, whereas for $V_f > 50\%$, the impact toughness is nearly constant. A slight increase from 0.79 to 1.37 kJ/m^2 is even detected when V_f further increases. The same trend has been reported by Lewandowski et al.[130] for a partially devitrified Zr-based metallic glass (Vit-1). With increasing volume fraction of crystals, the impact toughness decreases to very low values ($G < 10$ kJ/m^2). In both cases, no significant effect of the second phase on the impact toughness is detected below a critical volume fraction of micrometer-sized dendritic crystalline phase or beyond a critical volume fraction of nanocrystalline phases. This critical volume fraction (around 40–50%) is consistent with the one determined for ductility improvement/embrittlement. When the fracture energy is high, the ductility is enhanced whereas a low fracture energy induces brittleness. As for monolithic BMGs, the fracture energy can be correlated with the μ/B ratio.[128] When increasing crystallization is induced in a Zr–Ti–Cu–Ni–Be glass, the fracture energy decreases from 74 to 0.4 kJ/m^2 while the μ/B-ratio increases from 0.324 to 0.411.[128,130]

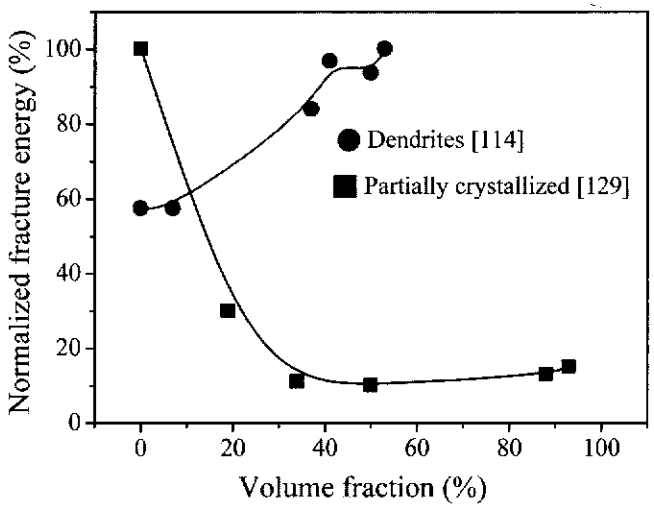

FIG. 11. Fracture energy (kJ/m^2) for a $La_{86-y}Al_{14}(Cu, Ni)_y$ (y = 12 to 24) glassy matrix/dendrite composite[114] and a partially devitrified $La_{55}Al_{25}Cu_{10}Ni_5Co_5$ BMG.[129]

IV. FRACTURE

A. Fracture angle

Fracture in metallic glasses occurs along the maximum shear stress plane at a critical shear stress τ_0. Bulk metallic glasses undergo fracture at a plane of 45° according to the Tresca yield criterion[121] in compression or in tension because of extensive shear localization and shearing off along the maximum shear stress plane. However, extensive studies[131–135] have shown that the fracture plane of metallic glasses deviates from this criterion. In compression, the measured angle generally ranges between 40° and 43° whereas in tension, it is usually between 50° and 60°.[131] Such a deviation from the maximum shear stress plane suggests that the normal stress (σ_C or σ_T) should be taken into account, which is in agreement with the Mohr–Coulomb model already mentioned for the yield asymmetry.[131] The critical shear stress for both shear compressive and tensile failure is then given by

$$\tau_c = \tau_0 + \mu_c\sigma_c \text{ (for compression)},$$

$$\tau_T = \tau_0 - \mu_T\sigma_T \text{ (for tension)},$$

where μ_C and μ_T are two constants for compression and tension.

The results on the fracture angle measurements for BMG composites are less uniform than for monolithic BMGs. In most cases, fracture occurs in a shear mode, and the fracture angle is similar to the one measured for comparable single-phase BMGs.[25,110] However, an enhanced contribution of the normal stress in compression, with a fracture angle around 31–33° has been reported for a Zr-based BMG ($Zr_{52.25}Cu_{28.5}Ni_{4.75}Al_{9.5}Ta_5$) containing Ta-rich precipitates.[132] Normal tensile fracture, with a fracture plane perpendicular to the tensile axis, occurs in cases of partially crystallized $Zr_{52.5}Ni_{14.6}Al_{10}Cu_{17.9}Ti_5$[131] and for La-based dendrite composites.[114] For this latter alloy system, even monolithic BMGs break with this fracture mode. Normal tensile fracture is attributed to low tensile fracture strength and to the main contribution of the crystalline phase to the fracture mode.[131] Some examples of compressive specimens breaking into multiple pieces have also been reported by Zhang et al.[131] At last, a mixture of shear fracture and delamination has been reported for ex situ composites containing filaments. Here, delamination becomes more and more important with increasing volume fraction of fibers.[52] Therefore, the fracture angle is

the result of a competitive process between shear, distensile, and normal tensile fracture depending on the loading mode and the microstructural features.

B. Fracture surfaces

The typical fracture surface of bulk metallic glasses loaded under compression displays a veinlike structure characteristic of a pure shear fracture mode.[19,131,134–136] This pattern is attributed to local softening or melting inside the shear band induced by the high elastic energy release upon instantaneous fracture.[135] For some BMGs, the veinlike structure coexists with riverlike patterns and smooth areas under uniaxial compression,[134] as depicted in Fig. 12. In this case, the fracture surface is covered by a riverlike pattern, intermittent smooth featureless regions, and a vein pattern. The origin of such morphology on the fracture surface has been described in Ref. 134. Besides the appearance of the vein pattern on the fracture surfaces of BMGs, the formation of riverlike patterns is due to the effect of the normal stress, which acts locally on a shear plane. The intermittent smooth regions form when a high rate of crack propagation is locally established after overcoming the threshold imposed by a crystalline particle.[134] The typical fracture surface of BMGs loaded in tension is quite different. Besides the veinlike pattern, it exhibits featureless round cores, which are generated by the normal stress acting on the shear plane.[135]

The fracture surfaces of composites are more complex. A mixture of different features can be observed the proportions of which depend on the volume fraction of the crystalline phase. Two cases have to be distinguished. When V_f increases and enhances the ductility of the composite, a mixture of veinlike features and highly rough surfaces with extensive local melting is observed in compression.[129,132,133] The length scale and area fraction of the veinlike structure decrease when the amount of crystalline phase increases. When the sample is loaded in tension[114] or in compression under dynamic conditions,[25] dimples are also observed. The lateral surfaces of the deformed samples show multiple shear bands parallel to the direction of the fracture plane.[134] With increasing V_f, the shear bands become more dense, and secondary shear bands form, induced by branching of the main shear bands and perpendicular to them.[132]

As the addition of a crystalline phase leads to embrittlement, the fracture surface usually consists of a mixture with a veinlike pattern, rough areas, and eventually honeycomblike features.[101,137] When V_f increases, the area covered by the veinlike morphology decreases, more microcracks and microvoids appear essentially along the shear bands and at the matrix/crystalline interface, and the shear band density on the lateral surface decreases.[110] In all the cases, shear bands, and then cracks, propagate through the glassy matrix and interact in different ways with the crystalline phase: either they move around or cut through the particles.[132]

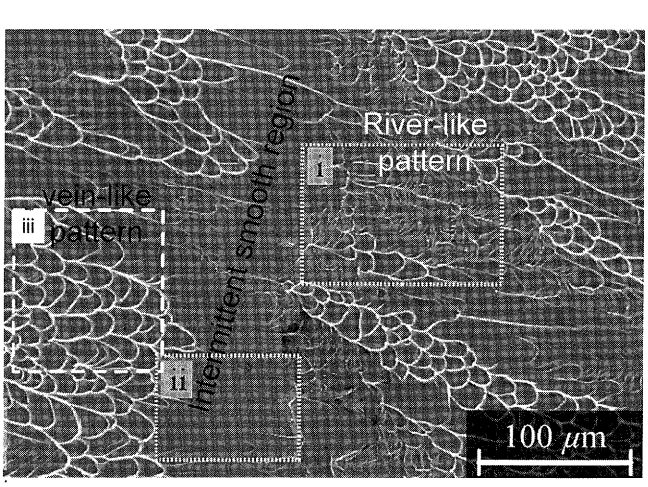

FIG. 12. Fractographic features appeared on $Zr_{61}Ti_4Nb_4Cu_{14}Ni_9Al_9$ BMG under compression showing the coexistence of riverlike pattern (frame i), intermittent smooth regions (frame ii), and typical veinlike pattern (frame iii).[134]

V. DEFORMATION AND FRACTURE MECHANISMS

A. Monolithic bulk metallic glasses

Monolithic BMGs exhibit only limited macroscopic plastic flow due to the formation of highly localized shear bands under loading.[23] The shear localization is a result of a rapid dilation accompanying the high-rate shear deformation of short-range ordered clusters.[138,139] Spreading of such localized shearing events occurs around shear transformation zones (STZs)[138,139] and creates free volume.[140] Localized shear transformations along certain preferred directions (i.e., along the direction of the maximum shear stress) create microstructural shear bands. Accumulation of free volume inside the shear bands decreases the viscosity, which finally appears as strain softening/thermal softening.[23] Due to local softening in the shear band, the region inside the shear band(s) deforms more easily than the rest of the sample.[23] Therefore, the softening in the shear bands leads to further plastic flow, and only a few shear bands have to be activated, leading to catastrophic failure soon after yielding.

B. BMG/nanocrystal composites containing quasicrystals or intermetallic compounds

The mechanical properties described above show that: (i) crystals have a strengthening effect on the glassy matrix as shown by hardness measurements, (ii) there is a critical volume fraction of (quasi)crystalline phase for which a ductile-to-brittle transition is observed, and (iii) nanocrystals[64] are more efficient than micrometer-sized particles for improving the mechanical properties.

Because nanoscale particles are free of defects (especially free of dislocations), the nano(quasi)crystals obtained either by partial devitrification or by quenching constitute a hard and nondeformable phase, as typically assumed.[64,141] Below the critical volume fraction, the nanocrystals are isolated and homogeneously distributed inside the matrix. Because their size is smaller than the shear band spacing, they increase the resistance to flow deformation by increasing the viscosity inside the shear band.[64,140] The glassy matrix hardens, which leads to a higher strength, and shear band propagation is retarded, thus enhancing the ductility. The nanocrystals seem to have no effect on crack initiation, and the deformation is still controlled by the amorphous matrix. Beyond the critical volume fraction, agglomerates of particles/crystals occur.[64,141,142] Thus, microstructural length scale becomes coarser than the shear band spacing. Stress concentrations appear at the interface between the crystals and the matrix and lead to the formation of microcracks, which accelerate the development of a long crack.[135] The flowability of the matrix decreases and the deformation becomes mainly controlled by the crystalline phase. The same process occurs when the size of the crystallites is too large (typically in the micrometer range).

C. BMG/ductile dendrites composites

The deformation mechanism of BMG/ductile β–Zr/Ti/Nb/Ta dendrite composites can be described as follows.[25–28] In the first stage, the ductile dendritic phase begins to yield, and part of the load is transferred to the surrounding glassy matrix. Possibly because of the strong interface between the β-phase and the matrix, the load transfer causes early yielding of the composite. Just after yielding, primary shear bands are initiated and propagate inside the glassy phase until they are blocked by the dendrites.[143–145] The slip is transferred from the matrix to the dendrites, and secondary shear bands are initiated in another direction to accommodate the strain. With further increasing strain, multiplication of shear bands in both directions occurs. The propagation of the shear bands is further hindered by the β-phase. The shear bands first move around the dendrites, but for higher strain levels, they cut through the crystals. During this process, microcracks are nucleated along the shear bands or at the dendrite/matrix interface. The crack propagation follows the shear band propagation, and similar phenomena occur. Cracks move around the dendrites, cut through them, or are stopped by them. Whatever happens, the pathway through which the crack propagates increases, but its propagation rate is retarded. The macroscopic consequence is an enhanced ductility. According to the previous scenario, the contribution of the dendrites to the ductility mainly occurs via shear band multiplication, branching, and interaction. As mentioned before, for monolithic BMGs, the strain localization inside the shear bands induces softening, which leads to further plastic flow. Because of the strong interface between the crystalline phase and the matrix, the dendrites can accommodate the stress intensity within the shear band. This results in a decrease of the local temperature inside the shear band, which stops temporarily, leading to a hardening of the glassy matrix. The intrinsic deformation behavior of the dendrites is also important as dislocation slip and multiplication occur in the β-phase and lead to work hardening, which further enhances the ductility.[145]

However, as shown in Fig. 9(b), only the presence of an intrinsically ductile phase is not sufficient for significant plastic deformation. There has to be an effective interaction between the length scale of the shear band and the microstructural length scale of the dendrites.[60] When the volume fraction of crystals is too low or if the dendrites are too small to hinder shear band propagation, there are not enough interfaces to initiate new shear bands. To have a beneficial effect on the ductility, the size of the dendrites should be at least equivalent to the shear band spacing. Lee et al. have shown for a $La_{86-y}Al_{14}(Cu, Ni)_y$ (y = 12 to 24) BMG/dendrite composite that the shear band spacing is in the range of 5 to 20 μm.[114] When the volume fraction of the β-phase is too small, the interdendritic spacing is around 10–40 μm, the dendrites do not substantially affect the shear band propagation, and no effect on the macroscopic ductility is detected. For the critical volume fraction of dendrites, the interdendritic spacing is on the order of 2–8 μm, i.e., just a little bit smaller than the shear band spacing. Then efficient interaction between the shear bands and the dendrites occurs, leading to work hardening and plastic deformation.[144]

VI. DUCTILE BULK METALLIC GLASSES

Very recently, high-strength bulk metallic glasses with enhanced room temperature ductility have been developed.[146–149] The yield strength, maximum strength, and total strain before failure in compression of such BMGs are given in Table I. All the alloys exhibit very high yield strength, between 1272 and 1830 MPa, and a significantly improved ductility as the total true strain can reach up to 170% for binary $Pd_{81}Si_{19}$.[90] After the yield point, the stress level continues to increase, indicating a "work-hardening-like" behavior.[146,148,150] This phenomenon seems to be common to most of the BMGs exhibiting intrinsically enhanced ductility, as shown by the difference between the yield strength and the maximum flow stress (Table I). The observation of such macroscopic hardening under compression is presented for Cu-based[146] and Ti-based[151] glasses in Fig. 13(a). Scanning electron microscopy (SEM) observations of surfaces of deformed samples reveal a high density of shear bands,

TABLE I. Yield strength (σ_y), maximal flow stress (σ_{max}), and total strain (ϵ_f) for recently reported ductile BMG.

Alloy	σ_y (MPa)	σ_{max} (MPa)	ϵ_f (%)	Ref.
$Cu_{47.5}Al_{47.5}Al_5$	1547	2265	18	146
$Cu_{43}Zr_{43}Al_7Ag_7$	1500	1850	8	93
$Cu_{50}Zr_{50}$	1830	2550	9.6	155
$Ti_{45}Cu_{40}Ni_{7.5}Zr_5Sn_{2.5}$	...	...	16	151
$Pt_{57.5}Cu_{14.7}Ni_{5.3}P_{22.5}$	1400	1470	22.8	147
$Pd_{81}Si_{19}$	1309	2590	True 170	90
$Zr_{65}Al_{7.5}Ni_{10}Pd_{17.5}$	1594	1698	6.6	148
$Zr_{59}Ta_5Cu_{18}Ni_8Al_{10}$	1700	1700	6.8	112

which are organized in two networks[146]: primary shear bands, which are more or less parallel to the fracture plane, and secondary shear bands perpendicular to the previous ones. The shear band spacing can be very small (around 150–500 nm), as revealed by high resolution scanning electron microscopy.[146] Intersection and interaction between the two patterns of shear bands as well as multiple branching and bifurcation are found. Moreover, the shear bands are not straight in shape but display a wavy-passing pattern.[146]

Different reasons have been proposed to explain this intrinsic ductility of bulk metallic glasses: large Poisson's ratio,[147] nanocrystallization during deformation,[148,150] liquid phase separation,[90,91,93] the presence of distinct short- or medium-range order,[112,146] and the development of "glassy martensite"[152] or supercooled martensitic alloys.[153] According to Schroers et al.,[145] the large macroscopic plasticity is a consequence of a high Poisson's ratio (e.g., $\nu = 0.41$ for $Pt_{57.5}Cu_{14.7}Ni_{5.3}P_{22.5}$), which restricts crack nucleation and/or propagation. Indeed, for a large Poisson's ratio, the release of local stress concentrations is more likely to occur via shear deformation instead of crack nucleation. Saida et al.[148] have observed a nanoscale "bandlike" structure after deformation of a Zr–Al–Ni–Pd ductile alloy. The true stress–true strain curve clearly reveals a "macroscopic hardening," as presented in the inset of Fig. 13(b). This feature is claimed to result from structural segregation and preceeding nanocrystallization induced by a local temperature increase and concentration of the shear stress.[148] Because of the presence of the nanocrystals, the shear band propagation is suddenly suppressed, and the nanocrystalline particles are rearranged along the stationary shear bands.[141,142] An increase of the stress level is then necessary to further propagate the shear bands, which results macroscopically scale in a work hardening behavior. Phase separation in the liquid state[91,93] has also been suggested to be responsible for chemical short-range inhomogeneities. In this picture, the microstructure consists of small clusters 3–6 nm in size, which are distributed throughout the glass. Significant differences between the chemical composition of the

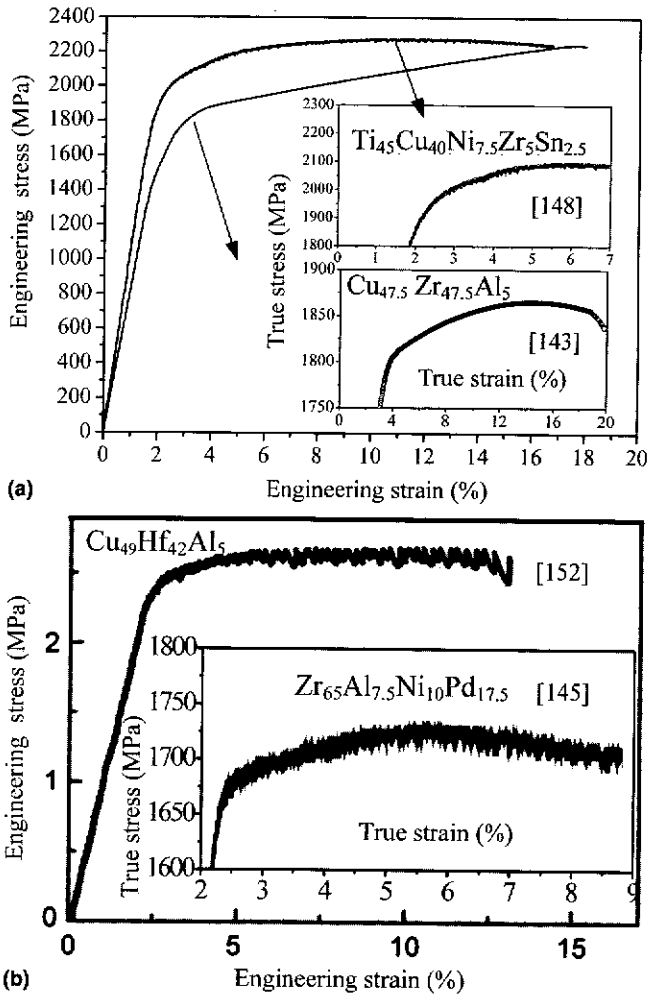

FIG. 13. Engineering stress–strain curves of a few work-hardenable ductile bulk metallic glasses under compression: (a) $Cu_{47.5}Zr_{47.5}Al_5$[146] and $Ti_{45}Cu_{40}Ni_{7.5}Zr_5Sn_{2.5}$;[151] (inset) true-stress-true-strain curves and (b) $Cu_{49}Hf_{42}Al_9$ BMG,[156] (inset) true stress–true strain curve of $Zr_{65}Al_{7.5}Ni_{10}Pd_{17.5}$ BMG.[148]

matrix and the clusters have been revealed by energy-dispersive x-ray analysis (EDX) and field ion microscopy (FIM).[93] Because of these different chemical compositions, different areas in the glass may require a different critical shear stress to initiate shear bands, and the nanoclusters can hinder and deflect their propagation. Finally, a $Zr_{48.5}Cu_{46.5}Al_5$ BMG composite containing a micrometer-scale martensite phase has also been found to exhibit 6.6% plastic deformation.[154]

It is interesting to notice that the $Zr_{65}Al_{7.5}Ni_{10}$-$Cu_{17.5-x}Pd_x$ monolithic BMG with $x = 5$[64] is macroscopically brittle and requires precipitation of 5–10 nm size nanocrystallites to obtain 8–10% plastic strain. On the other hand, a monolithic BMG ($x = 17.5$) shows large ductility and work hardening behavior[148] [inset in Fig. 13(b)]. The same holds for $Cu_{50}Zr_{50}$-base metallic glasses and glass matrix nano-composites.[146,149,154,155] Similarly, a large ductility and strain-hardening has also

been observed in a monolithic $Cu_{49}Hf_{42}Al_9$ BMG, as shown in Fig. 13(b).[156] The common feature of all these ductile bulk metallic glasses is that they are rather poor glass-forming alloys. It has recently been reported that an increase in Poisson's ratio is linked with a decrease of the glass-forming ability[157] pushing such alloys more toward fragile-type rather than strong glasses according to Angell's classification.[158] Fragile glasses can be viewed as a mixture of "solidlike" and "liquidlike" structural entities.[159] Upon deformation, the more liquidlike regions carry plasticity, similar to the dislocation motion in crystals.[159] The liquidlike and solidlike distinction indicates the possibility to find repeatable inelastic atomic-level structural changes associated with the transformation of liquidlike atomic environments into solidlike ones and vice versa.[160] In addition, an irreversible production of free volume due to external stress has been claimed to be the reason for work-hardening in amorphous material.[161]

VII. CONCLUSIONS AND FUTURE TRENDS

The wide range of superior mechanical properties of bulk metallic glasses and their composites renders a unique opportunity for developing new advanced materials, which can be exploited for a variety of engineering applications. The unique structure–property correlation of metallic glasses is of scientific as well as of industrial interest. A large number of glassy matrix composites with quasicrystalline, crystalline, and noncrystalline second phase dispersions on the nanometer–micrometer length scale have been produced either by solidification, mechanical alloying and consolidation, or a secondary treatment (e.g., annealing or severe plastic deformation) of amorphous precursors. Tailorable mechanical properties (strength, hardness, ductility, toughness) can be achieved from either in situ or ex situ BMG composites by adopting proper processing techniques and tuned-in compositions to change the size and the volume fraction of the second phase dispersions. However, fine tuning to optimize the properties requires further investigations concerning alloy design and processing conditions. Monolithic bulk metallic glasses do not show macroscopic plastic deformability, but recent advances in structurally inhomogeneous glasses with high Poisson's ratio open a new door for "processing for unique properties" of bulk metallic glasses. However, the deformation mechanisms of such BMGs are still rather poorly understood. Here a lot of work has to be done to elucidate the mechanisms responsible for the observed ductility enhancement. This not only has to involve in-depth structural investigations of as-prepared and deformed specimens, but also systematic testing under different loading conditions and a thorough analysis of shear band propagation and, finally, of the fracture behavior. Along this line, macroscopic mechanical testing has to be linked with an appropriate description of the short- and medium-range order of the glass incorporating nanoscale inhomogeneties to gain a better model-based description and a clear picture of the underlying mechanism of plastic deformation. Nevertheless, the high elastic strain and high strength, good corrosion resistance, and high fracture toughness of BMGs and their composites, at least in some cases, give a very interesting perspective for the development of new materials for structural and functional applications, which can replace conventional crystalline metals and alloys.

ACKNOWLEDGMENTS

The authors are grateful to M. Frey, H. Grahl, R. Günther, H. Kempe, U. Kunz, H.J. Klauss, H. Lehmann, H.G. Lindenkreuz, C. Mickel, and C. Wasmund for technical assistance and to A. Argon, F. Baier, M. Baricco, M.D. Baró, R. Busch, M. Calin, A. Concustell, E. Fleury, A. Gebert, A.L. Greer, A. Güth, G. He, M. Heilmaier, A. Inoue, M.H. Lee, J.J. Lewandowski, M. Li, W.L. Johnson, K.B. Kim, D.H. Kim, U. Kühn, W. Löser, N. Mattern, S.K. Roy, D.J. Sordelet, K. Samwer, L. Schultz, S. Scudino, J. Schroers, M. Stoica, S. Venkataraman, W.H. Wang, T.G. Woodcock, L.Q. Xing, W. Xu, A.R. Yavari, P. Yu, and Z.F. Zhang for stimulating discussions. Financial support provided by the European Union within the framework of the research and training networks on Bulk Metallic Glasses (HPRN-CT-2000-00033) and Ductile BMG Composites (MRTN-CT-2003-504692), as well as by the Deutscher Akademischer Austauschdienst (DAAD), the Deutsche Forschungsgemeinschaft (DFG) (Grant Nos. EC 111/10, EC 111/12, EC 111/15), and the Alexander von-Humboldt Foundation, are gratefully acknowledged.

REFERENCES

1. J. Kramer: Nonconducting modifications of metals. *Ann. Physik (Berlin, Germany)* **19,** 37 (1934).
2. A. Brenner, D.E. Couch, and E.K. Williams: Electrodeposition of alloys of phosphorus with nickel or cobalt. *J. Res. Nat. Bur. Stand.* **44,** 109 (1950).
3. W. Buckel and R. Hilsch: On the superconductivity of copper sulfide. *Z. Physik* **128,** 324 (1950), (in German).
4. W. Buckel and R. Hilsch: Superconductivity and resistivity of tin with lattice distortion. *Z. Physik* **131,** 420 (1952), (in German).
5. W. Klement, R.H. Willens, and P. Duwez: Non-crystalline structure in solidified gold-silicon alloys. *Nature* **187,** 869 (1960).
6. P. Duwez, R.H. Willens, and R.C. Crewdson: Amorphous phase in palladium-silicon alloys. *J. Appl. Phys.* **36,** 2267 (1965).
7. H.S. Chen: Thermodynamic considerations on formation and stability of metallic glasses. *Acta Metall.* **22,** 1505 (1974).
8. A.J. Drehman, A.L. Greer, and D. Turnbull: Bulk formation of a metallic-glass $Pd_{40}Ni_{40}P_{20}$. *Appl. Phys. Lett.* **41,** 716 (1982).
9. A. Inoue, T. Zhang, and T. Masumoto: Al–La–Ni amorphous-alloys with a wide supercooled liquid region. *Mater. Trans., JIM* **30,** 965 (1989).

10. A. Inoue, T. Nakamura, N. Nishiyama, and T. Masumoto: Mg–Cu–Y bulk amorphous-alloys with high-tensile strength produced by a high-pressure die-casting method. *Mater. Trans., JIM* **33,** 937 (1992).
11. A. Peker and W.L. Johnson: A highly processable metallic glass, $Zr_{41.2}Ti_{13.8}Cu_{12.5}Ni_{10.0}Be_{22.5}$. *Appl. Phys. Lett.* **63,** 2342 (1993).
12. A. Inoue, T. Zhang, N. Nishiyama, K. Ohba, and T. Masumoto: Preparation of 16 mm diameter rod of amorphous $Zr_{65}Al_{7.5}Ni_{10}Cu_{17.5}$ alloy. *Mater. Trans., JIM* **34,** 1234 (1993).
13. A. Gebert, K. Buchholz, A. Leonhard, K. Mummert, J. Eckert, and L. Schultz: Investigations on the electrochemical behaviour of Zr-based bulk metallic glasses. *Mater. Sci. Eng., A* **267,** 294 (1999).
14. L.A. Davis: Hardness/strength ratio of metallic glasses. *Scripta Metall.* **9,** 431 (1975).
15. P.E. Donovan: Plastic-flow and fracture of $Pd_{40}Ni_{40}P_{20}$ metallic glass under an indenter. *J. Mater. Sci.* **24,** 523 (1989).
16. W.L. Johnson: Bulk glass-forming metallic alloys: Science and technology. *MRS Bull.* **24,** 42 (1999).
17. R.D. Conner, A.J. Rosakis, W.L. Johnson, and D.M. Owen: Fracture toughness determination for a beryllium-bearing bulk metallic glass. *Scripta Mater.* **37,** 1373 (1997).
18. P. Wesseling, T.G. Nieh, W.H. Wang, and J.J. Lewandowski: Preliminary assessment of flow, notch toughness, and high temperature behavior of $Cu_{60}Zr_{20}Hf_{10}Ti_{10}$ bulk metallic glass. *Scripta Mater.* **51,** 151 (2004).
19. X.K. Xi, D.Q. Zhao, M.X. Pan, W.H. Wang, Y. Wu, and J.J. Lewandowski: Fracture of brittle metallic glasses: Brittleness or plasticity. *Phys. Rev. Lett.* **94,** 125510 (2005).
20. H. Kimura and T. Masumoto: Deformation and fracture of an amorphous Pd–Cu–Si alloy in v-notch bending tests II ductile-brittle transition. *Acta Metall.* **28,** 1677 (1980).
21. C.H. Shek, G.M. Lin, K.L. Lee, and J.K.L. Lai: Fractal fracture of amorphous $Fe_{46}Ni_{32}V_2Si_{14}B_6$ alloy. *J. Non-Cryst. Solids* **224,** 244 (1998).
22. M.F. Ashby and A.L. Greer: Metallic glasses as structural materials. *Scripta Mater.* **54,** 321 (2006).
23. J.J. Lewandowski and A.L. Greer: Temperature rise at shear bands in metallic glasses. *Nat. Mater.* **5,** 15 (2006).
24. H.A. Bruck, T. Christman, A.J. Rosakis, and W.L. Johnson: Quasistatic constitutive behavior of $Zr_{41.2}Ti_{13.8}Cu_{12.5}Ni_{10.0}Be_{22.5}$ bulk amorphous alloys. *Scripta Metall. Mater.* **30,** 429 (1994).
25. C.C. Hays, C.P. Kim, and W.L. Johnson: Microstructure controlled shear band pattern formation and enhanced plasticity of bulk metallic glasses containing in situ formed ductile phase dendrite dispersions. *Phys. Rev. Lett.* **84,** 2901 (2000).
26. U. Kühn, J. Eckert, N. Mattern, and L. Schultz: ZrNbCuNiAl bulk metallic glass matrix composites containing dendritic bcc phase precipitates. *Appl. Phys. Lett.* **80,** 2478 (2002).
27. J. Eckert, U. Kühn, N. Mattern, G. He, and A. Gebert: Structural bulk metallic glasses with different length-scale of constituent phases. *Intermetallic* **10,** 1183 (2002).
28. H. Ma, J. Xu, and E. Ma: Mg-based bulk metallic glass composites with plasticity and high strength. *Appl. Phys. Lett.* **83,** 2793 (2003).
29. C.C. Koch, O.B. Cavin, C.G. Mckamey, and J.O. Scarbrough: Preparation of amorphous $Ni_{60}Nb_{40}$ by mechanical alloying. *Appl. Phys. Lett.* **43,** 1017 (1983).
30. J. Eckert: Mechanical alloying of highly processable glassy alloys. *Mater. Sci. Eng., A* **226,** 364 (1997).
31. S.A. Miller and R.J. Murphy: Gas-water atomization process for producing amorphous powders. *Scripta Metall.* **13,** 673 (1979).
32. F.E. Luborsky: *Amorphous Metallic Alloys* (Butterworths, London, UK, 1983).
33. L. Schultz and J. Eckert: Mechanically alloyed glassy metals, in *Glassy Metals III: Amorphization Techniques, Catalysis, Electronic and Ionic Structure*, edited by H. Beck, and H.J. Güntherodt (Springer-Verlag, Berlin, Germany, 1994), p. 70.
34. J. Eckert, L. Schultz, E. Hellstern, and K. Urban: Glass-forming range in mechanically alloyed Ni-Zr and the influence of the milling intensity. *J. Appl. Phys.* **64,** 3224 (1988).
35. J. Eckert, M. Seidel, N. Schlorke, A. Kübler, and L. Schultz: Solid state processing of bulk metallic glass forming alloys. *Mater. Sci. Forum* **235,** 23 (1997).
36. L.Q. Xing, J. Eckert, W. Löser, and L. Schultz: High-strength materials produced by precipitation of icosahedral quasicrystals in bulk Zr–Ti–Cu–Ni–Al amorphous alloys. *Appl. Phys. Lett.* **74,** 664 (1999).
37. L.Q. Xing, J. Eckert, W. Löser, L. Schultz, and D.M. Herlach: Crystallization behaviour and nanocrystalline microstructure evolution of a $Zr_{57}Cu_{20}Al_{10}Ni_8Ti_5$ bulk amorphous alloy. *Philos. Mag. A* **79,** 1095 (1999).
38. J. Saida, M. Matsushita, T. Zhang, A. Inoue, M.W. Chen, and T. Sakurai: Precipitation of icosahedral phase from a supercooled liquid region in $Zr_{65}Cu_{7.5}Al_{7.5}Ni_{10}Ag_{10}$ metallic glass. *Appl. Phys. Lett.* **75,** 3497 (1999).
39. N. Boucharat, R. Hebert, H. Rosner, R. Valiev, and G. Wilde: Nanocrystallization of amorphous $Al_{88}Y_7Fe_5$ alloy induced by plastic deformation. *Scripta Mater.* **53,** 823 (2005).
40. G. Wilde, N. Boucharat, G.P. Dinda, H. Rosner, and R.Z. Valiev: New routes for synthesizing massive nanocrystalline materials. *Mater. Sci. Forum* **503–504,** 425 (2006).
41. M.H. Lee, D.H. Bae, W.T. Kim, D.H. Kim, E. Rozhkova, P.B. Wheelock, and D.J. Sordelet: Synthesis of Ni-based bulk amorphous alloys by warm extrusion of amorphous powders. *J. Non-Cryst. Solids* **315,** 89 (2003).
42. Y. Kawamura, A. Inoue, K. Sasamori, A. Katoh, and T. Masumoto: High-strength crystalline aluminum-alloys produced from amorphous powder by a closed P/M processing. *Mater. Trans., JIM* **34,** 969 (1993).
43. J. Eckert, N. Schlorke-de Boer, B. Weiss, and L. Schultz: Mechanically alloyed Mg-based metallic glasses and metallic glass composites containing nanocrystalline particles. *Z. Metallkd.* **90,** 908 (1999).
44. J. Eckert, M. Seidel, A. Kübler, U. Klement, and L. Schultz: Oxide dispersion strengthened mechanically alloyed amorphous Zr–Al–Cu–Ni composites. *Scripta Mater.* **38,** 595 (1998).
45. J. Eckert, A. Kübler, and L. Schultz: Mechanically alloyed $Zr_{55}Al_{10}Cu_{30}Ni_5$ metallic glass composites containing nanocrystalline W particles. *J. Appl. Phys.* **85,** 7112 (1999).
46. J. Eckert: Mechanical behavior of nanocrystalline metals, in *Nanostructured Materials: Processing, Properties and Applications,* edited by C.C. Koch (William Andrews Publishing, Norwich, NY, 2002), p. 423.
47. H. Choi-Yim, R.D. Conner, F. Szuecs, and W.L. Johnson: Processing, microstructure and properties of ductile metal particulate reinforced $Zr_{57}Nb_5Al_{10}Cu_{15.4}Ni_{12.6}$ bulk metallic glass composites. *Acta Mater.* **50,** 2737 (2002).
48. H. Choi-Yim, R. Busch, U. Köster, and W.L. Johnson: Synthesis and characterization of particulate reinforced $Zr_{57}Nb_5Al_{10}Cu_{15.4}Ni_{12.6}$ bulk metallic glass composites. *Acta Mater.* **47,** 2455 (1999).
49. R.D. Conner, H. Choi-Yim, and W.L. Johnson: Mechanical properties of $Zr_{57}Nb_5Al_{10}Cu_{15.4}Ni_{12.6}$ metallic glass matrix particulate composites. *J. Mater. Res.* **14,** 3292 (1999).
50. R.B. Dandliker, R.D. Conner, and W.L. Johnson: Melt infiltration casting of bulk metallic-glass matrix composites. *J. Mater. Res.* **13,** 2896 (1998).
51. C.P. Kim, R. Busch, A. Masuhr, H. Choi-Yim, and W.L. Johnson:

Processing of carbon-fiber-reinforced $Zr_{41.2}Ti_{13.8}Cu_{12.5}Ni_{10.0}Be_{22.5}$ bulk metallic glass composites. *Appl. Phys. Lett.* **79,** 1456 (2001).
52. R.D. Conner, R.B. Dandliker, and W.L. Johnson: Mechanical properties of tungsten and steel fiber reinforced $Zr_{41.25}Ti_{13.75}Cu_{12.5}Ni_{10}Be_{22.5}$ metallic glass matrix composites. *Acta Mater.* **46,** 6089 (1998).
53. H. Choi-Yim and W.L. Johnson: Bulk metallic glass matrix composites. *Appl. Phys. Lett.* **71,** 3808 (1997).
54. Z. Bian, R.J. Wang, W.H. Wang, T. Zhang, and A. Inoue: Carbon-nanotube-reinforced Zr-based bulk metallic glass composites and their properties. *Adv. Func. Mater.* **14,** 55 (2004).
55. A. Inoue, H. Kimura, K. Sasamori, and T. Masumoto: High mechanical strength of Al-(V,Cr,Mn)-(Fe,Co,Ni) quasicrystalline alloys prepared by rapid solidification. *Mater. Trans., JIM* **37,** 1287 (1996).
56. A. Inoue and H.M. Kimura: Development of high-strength aluminum-based alloys by synthesis of new multicomponent quasicrystals, in *Quasicrystals,* edited by J.M. Dubois, P.A. Thiel, A.P. Tsai, and K. Urban (Mater. Res. Soc. Symp. Proc. **553,** Warrendale, PA, 1999), p. 495.
57. H.M. Kimura, A. Inoue, K. Sasamori, and T. Masumoto: Microstructure of rapidly solidified Al–V–Ce–M (M = Fe, Co, or Ni) high-strength alloys containing high-volume fraction of fine icosahedral precipitation. *Mater. Trans., JIM* **36,** 1004 (1995).
58. U. Kühn, J. Eckert, N. Mattern, and L. Schultz: As-cast quasicrystalline phase in a Zr-based multicomponent bulk alloy. *Appl. Phys. Lett.* **77,** 3176 (2000).
59. F.Q. Guo, H.J. Wang, S.J. Poon, and G.J. Shiflet: Ductile titanium-based glassy alloy ingots. *Appl. Phys. Lett.* **86,** 091907 (2005).
60. J. Eckert, N. Mattern, M. Zinkevitch, and M. Seidel: Crystallization behavior and phase formation in Zr–Al–Cu–Ni metallic glass containing oxygen. *Mater. Trans.* **39,** 623 (1998).
61. A. Gebert, J. Eckert, and L. Schultz: Effect of oxygen on phase formation and thermal stability of slowly cooled $Zr_{65}Al_{7.5}Cu_{7.5}Ni_{10}$ metallic glass. *Acta Mater.* **46,** 5475 (1998).
62. A. Inoue, T. Zhang, M.W. Chen, T. Sakurai, J. Saida, and M. Matsushita: Ductile quasicrystalline alloys. *Appl. Phys. Lett.* **76,** 967 (2000).
63. A. Leonhard, L.Q. Xing, M. Heilmaier, A. Gebert, J. Eckert, and L. Schultz: Effect of crystalline precipitations on the mechanical behavior of bulk glass forming Zr-based alloys. *Nanostruct. Mater.* **10,** 805 (1998).
64. K. Hajlaoui, A.R. Yavari, J. Das, and G. Vaughan: Ductilization of BMGs by optimization of nanoparticale dispersion. *J. Alloys Compd.* (in press).
65. J. Saida, H. Kato, A. Inoue, and M. Ohnuma: Novel nanostructure and deformation behavior in rapidly quenched Cu–(Zr or Hf)–Ti alloys. *Adv. Eng. Mater.* **7,** 39 (2005).
66. M. Kasai, J. Saida, M. Matsushita, T. Osuna, E. Matsubara, and A. Inoue: Structure and crystallization of rapidly quenched Cu–(Zr or Hf)–Ti alloys containing nanocrystalline particles. *J. Phys. Condens. Matter* **14,** 13867 (2002).
67. M. Calin, J. Eckert, and L. Schultz: Improved mechanical behavior of Cu-Ti-based bulk metallic glass by in situ formation of nanoscale precipitates. *Scripta Mater.* **48,** 653 (2003).
68. J.Z. Jiang, J. Saida, H. Kato, T. Ohsuna, and A. Inoue: Is $Cu_{60}Ti_{10}Zr_{30}$ a bulk glass-forming alloy? *Appl. Phys. Lett.* **82,** 4041 (2003).
69. G. He, W. Löser, J. Eckert, and L. Schultz: Enhanced plasticity in a Ti-based bulk metallic glass-forming alloy by in situ formation of a composite microstructure. *J. Mater. Res.* **17,** 3015 (2002).
70. Z. Bian, J. Ahmad, W. Zhang, and A. Inoue: In situ formed $(Cu_{0.6}Zr_{0.25}Ti_{0.15})_{93}Nb_7$ bulk metallic glass composites. *Mater. Trans., JIM* **45,** 2346 (2004).
71. Z. Bian, H. Kato, C.L. Qin, W. Zhang, and A. Inoue: Cu–Hf–Ti–Ag–Ta bulk metallic glass composites and their properties. *Acta Mater.* **53,** 2037 (2005).
72. J. Eckert, U. Kühn, J. Das, S. Scudino, and N. Radtke: Nanostructured composite materials with improved deformation behavior. *Adv. Eng. Mater.* **7,** 587 (2005).
73. J. Eckert, J. Das, and K.B. Kim: *Nanostructured Composites: Ti-base alloys, Encyclopedia of Nanoscience and Nanotechnology* (Marcel Dekker, NY, 2006)
74. G. He, J. Eckert, W. Löser, and L. Schultz: Novel Ti-base nanostructure-dendrite composite with enhanced plasticity. *Nat. Mater.* **2,** 33 (2003).
75. G. He, J. Eckert, and W. Löser: In situ formed Ti–Cu–Ni–Sn–Ta nanostructure-dendrite composite with large plasticity. *Acta Mater.* **51,** 5223 (2003).
76. G. He, J. Eckert, W. Löser, and M. Hagiwara: Composition dependence of the microstructure and the mechanical properties of nano/ultrafine-structured Ti–Cu–Ni–Sn–Nb alloys. *Acta Mater.* **52,** 3035 (2004).
77. J. Das, W. Löser, U. Kühn, J. Eckert, S.K. Roy, and L. Schultz: High-strength Zr–Nb–(Cu,Ni,Al) composites with enhanced plasticity. *Appl. Phys. Lett.* **82,** 4690 (2003).
78. J. Das, A. Güth, H-J. Klauss, C. Mickel, W. Löser, J. Eckert, S.K. Roy, and L. Schultz: Effect of casting conditions on microstructure and mechanical properties of high-strength $Zr_{73.5}Nb_9Cu_7Ni_1Al_{9.5}$ in situ composites. *Scripta Mater.* **49,** 1189 (2003).
79. S. Scudino, J. Das, M. Stoica, K.B. Kim, M. Kusy, and J. Eckert: High strength hexagonal structured dendritic phase reinforced Zr–Ti–Ni bulk alloy with enhanced ductility. *Appl. Phys. Lett.* **88,** 201920 (2006).
80. H. Choi-Yim, R.D. Conner, and W.L. Johnson: In situ composite formation in the Ni–(Cu)–Ti–Zr–Si system. *Scripta Mater.* **53,** 1467 (2005).
81. K.B. Kim, S. Yi, H. Choi-Yim, J. Das, W.L. Johnson, and J. Eckert: Interfacial instability-driven amorphization/nanocrystallization in a bulk $Ni_{45}Cu_5Ti_{33}Zr_{16}Si_1$ alloy during solidification. *Phys. Rev. B* **72,** 092102 (2005).
82. J. Das, S.K. Roy, W. Löser, J. Eckert, and L. Schultz: Novel in situ nanostructure-dendrite composites in Zr-base multicomponent alloy system. *Mater. Manuf. Proc.* **19,** 423 (2004).
83. C. Fan, R.T. Ott, and T.C. Hufnagel: Metallic glass matrix composite with precipitated ductile reinforcement. *Appl. Phys. Lett.* **81,** 1020 (2002).
84. J.C. Lee, Y.C. Kim, J.P. Ahn, and H.S. Kim: Enhanced plasticity in a bulk amorphous matrix composite: Macroscopic and microscopic viewpoint studies. *Acta Mater.* **53,** 129 (2005).
85. C.P.P. Chou and D. Turnbull: Transformation behavior of Pd–Au–Si metallic glasses. *J. Non-Cryst. Solids* **17,** 169 (1975).
86. H.S. Chen: Glass temperature, formation and stability of Fe, Co, Ni, Pd and Pt based glasses. *Mater. Sci. Eng.* **23,** 151 (1976).
87. R. Busch, S. Schneider, A. Peker, and W.L. Johnson: Decomposition and primary crystallization in undercooled $Zr_{41.2}Ti_{13.8}Cu_{12.5}Ni_{10.0}Be_{22.5}$ melts. *Appl. Phys. Lett.* **67,** 1544 (1995).
88. W. Liu, W.L. Johnson, S. Schneider, U. Geyer, and P. Thiyagarajan: Small-angle x-ray-scattering study of phase separation and crystallization in the bulk amorphous $Mg_{62}Cu_{25}Y_{10}Li_3$ alloy. *Phys. Rev. B* **59,** 11755 (1999).
89. M.K. Miller, D.J. Larson, R.B. Schwarz, and Y. He: Decomposition in $Pd_{40}Ni_{40}P_{20}$ metallic glass. *Mater. Sci. Eng., A* **250,** 141 (1998).

90. K.F. Yao, F. Ruan, Y.Q. Yang, and N. Chen: Superductile bulk metallic glass. *Appl. Phys. Lett.* **88,** 122106 (2006).
91. K.B. Kim, J. Das, F. Baier, M.B. Tang, W.H. Wang, and J. Eckert: Heterogeneity of a $Cu_{47.5}Zr_{47.5}Al_5$ bulk metallic glass. *Appl. Phy. Lett.* **88,** 051911 (2006).
92. M.K. Miller, S.C. Glade, and W.L. Johnson: Phase separation in $Cu_{47}Ti_{33}Zr_{11}Ni_8Si_1$ surface and interface analysis. *Surf. Interface Anal.* **36,** 598 (2004).
93. J.C. Oh, T. Ohkubo, Y.C. Kim, E. Fleury, and K. Hono: Phase separation in $Cu_{43}Zr_{43}Al_7Ag_7$ bulk metallic glass. *Scripta Mater.* **53,** 165 (2005).
94. E.S. Park and D.H. Kim: Phase separation and enhancement of plasticity in Cu–Zr–Al–Y bulk metallic glasses. *Acta Mater.* **54,** 2597 (2006).
95. B.J. Park, H.J. Chang, D.H. Kim, W.T. Kim, K. Chattopadhyay, T.A. Abinandanan, and S. Bhattacharyya: Phase separating bulk metallic glass: A hierarchical composite. *Phys. Rev. Lett.* **96,** 245503 (2006).
96. N. Mattern, U. Kuhn, A. Gebert, T. Gemming, M. Zinkevich, H. Wendrock, and L. Schultz: Microstructure and thermal behavior of two-phase amorphous Ni–Nb–Y alloy. *Scripta Mater.* **53,** 271 (2005).
97. H. Choi-Yim, D.H. Xu, M.L. Lind, J.F. Löffler, and W.L. Johnson: Structure and mechanical properties of bulk glass-forming Ni–Nb–Sn alloys. *Scripta Mater.* **54,** 187 (2006).
98. B. Lohwongwatana, J. Schroers, and W.L. Johnson: Strain rate induced crystallization in bulk metallic glass-forming liquid. *Phys. Rev. Lett.* **96,** 075503 (2006).
99. A. Inoue: Bulk glassy and nonequilibrium crystalline alloys by stabilization of supercooled liquid: Fabrication, functional properties and application. *Proc. Jpn. Acad.* **81B,** 156 (2005).
100. H. Li, G. Subhash, L.J. Kecskes, and R.J. Dowding: Mechanical behavior of tungsten preform reinforced bulk metallic glass composites. *Mater. Sci. Eng., A* **403,** 134 (2005).
101. H.M. Fu, H.F. Zhang, H. Wang, Q.S. Zhang, and Z.Q. Hu: Synthesis and mechanical properties of Cu-based bulk metallic glass composites containing in-situ TiC particles. *Scripta Mater.* **52,** 669 (2005).
102. Y.K. Xu, H. Ma, J. Xu, and E. Ma: Mg-based bulk metallic glass composites with plasticity and gigapascal strength. *Acta Mater.* **53,** 1857 (2005).
103. H.K. Lim, E.S. Park, J.S. Park, W.T. Kim, and D.H. Kim: Fabrication and mechanical properties of WC particulate reinforced $Cu_{47}Ti_{33}Zr_{11}Ni_6Sn_2Si_1$ bulk metallic glass matrix composites. *J. Mater. Sci.* **40,** 6127 (2005).
104. H. Kato, K. Yubuta, D.V. Louzguine, A. Inoue, and H.S. Kim: Influence of nanoprecipitation on strength of $Cu_{60}Zr_{30}Ti_{10}$ glass containing μm–ZrC particle reinforcements. *Scripta Mater.* **51,** 577 (2004).
105. J.S.C. Jang, L.J. Chang, J.H. Young, J.C. Huang, and C.Y.A. Tsao: Synthesis and characterization of the Mg-based amorphous/nano ZrO_2 composite alloy. *Intermetallics* **14,** 945 (2006).
106. H. Choi-Yim, J. Schroers, and W.L. Johnson: Microstructures and mechanical properties of tungsten wire/particle reinforced $Zr_{57}Nb_5Al_{10}Cu_{15.4}Ni_{12.6}$ metallic glass matrix composites. *Appl. Phys. Lett.* **80,** 1906 (2002).
107. H.M. Fu, H. Wang, H.F. Zhang, and Z.Q. Hu: In situ TiB-reinforced Cu-based bulk metallic glass composites. *Scripta Mater.* **54,** 1961 (2006).
108. A. Inoue, T. Zhang, S. Ishihara, J. Saida, and M. Matsushita: Preparation and mechanical properties of nanoquasicrystalline base bulk alloys. *Scripta Mater.* **44,** 1615 (2001).
109. L.Q. Xing, C. Bertrand, J.P. Dallas, and M. Cornet: Nanocrystal evolution in bulk amorphous $Zr_{57}Cu_{20}Al_{10}Nb_8Ti_5$ alloy and its mechanical properties. *Mater. Sci. Eng., A* **241,** 216 (1998).
110. Z. Bian, G.L. Chen, G. He, and X.D. Hui: Microstructure and ductile-brittle transition of as-cast Zr-based bulk glass alloys under compressive testing. *Mater. Sci. Eng., A* **316,** 135 (2001).
111. R.T. Ott, C. Fan, J. Li, and T.C. Hufnagel: Structure and properties of Zr–Ta–Cu–Ni–Al bulk metallic glasses and metallic glass matrix composites. *J. Non-Cryst. Solids.* **317,** 158 (2003).
112. L.Q. Xing, Y. Li, K.T. Ramesh, J. Li, and T.C. Hufnagel: Enhanced plastic strain in Zr-based bulk amorphous alloys. *Phys. Rev. B* **64,** 180201 (2001).
113. A.V. Sergueeva, N.A. Mara, J.D. Kuntz, E.J. Lavernia, and A.K. Mukherjee: Shear band formation and ductility in bulk metallic glass. *Philos. Mag.* **85,** 2671 (2005).
114. M.L. Lee, Y. Li, and C.A. Schuh: Effect of a controlled volume fraction of dendritic phases on tensile and compressive ductility in La-based metallic glass matrix composites. *Acta Mater.* **52,** 4121 (2004).
115. F. Szuecs, C.P. Kim, and W.L. Johnson: Mechanical properties of $Zr_{56.2}Ti_{13.8}Nb_{5.0}Cu_{6.9}Ni_{5.6}Be_{12.5}$ ductile phase reinforced bulk metallic glass composite. *Acta Mater.* **49,** 1507 (2001).
116. P. Wesseling, T.G. Nieh, W.H. Wang, and J.J. Lewandowski: Preliminary assessment of flow, notch toughness, and high temperature behavior of $Cu_{60}Zr_{20}Hf_{10}Ti_{10}$ bulk metallic glass. *Scripta Mater.* **51,** 151 (2004).
117. F.X. Liu, P.K. Liaw, G.Y. Wang, C.L. Chiang, D.A. Smith, P.D. Rack, J.P. Chu, and R.A. Buchanan: Specimen-geometry effects on mechanical behavior of metallic glasses. *Intermetallics* **14,** 1014 (2006).
118. U. Kühn, J. Eckert, N. Mattern, and L. Schultz: Microstructure and mechanical properties of slowly cooled Zr–Nb–Cu–Ni–Al composites with ductile bcc phase. *Mater. Sci. Eng., A* **375,** 322 (2004).
119. S. Cheng, J.A. Spencer, and W.W. Milligan: Strength and tension/compression asymmetry in nanostructured and ultrafine-grain metals. *Acta Mater.* **51,** 4505 (2003).
120. P.E. Donovan: A yield criterion for $Pd_{40}Ni_{40}P_{20}$ metallic glass. *Acta Metall.* **37,** 445 (1989).
121. G.E. Dieter: *Mechanical Metallurgy,* 3rd ed. (McGraw-Hill Book Company, London, UK, 1988), p. 330.
122. A.C. Lund and C.A. Schuh: Yield surface of a simulated metallic glass. *Acta Mater.* **51,** 5399 (2003).
123. Z.F. Zhang and J. Eckert: Unified tensile fracture criterion. *Phys. Rev. Lett.* **94,** 094301 (2005).
124. J. Eckert, A. Reger-Leonhard, B. Weiss, M. Heilmaier, and L. Schultz: Bulk nanostructured multicomponent alloys. *Adv. Eng. Mater.* **3,** 41 (2001).
125. T. Gloriant: Microhardness and abrasive wear resistance of metallic glasses and nanostructured composite materials. *J. Non-Cryst. Solids* **316,** 96 (2003).
126. A.L. Greer: Partially or fully devitrified alloys for mechanical properties. *Mater. Sci. Eng., A* **304,** 68 (2001).
127. Z.C. Zhong, X.Y. Jiang, and A.L. Greer: Microstructure and hardening of Al-based nanophase composites. *Mater. Sci. Eng., A* **226,** 531 (1997).
128. J.J. Lewandowski, W.H. Wang, and A.L. Greer: Intrinsic plasticity or brittleness of metallic glasses. *Philos. Mag. Lett.* **85,** 77 (2005).
129. N. Nagendra, U. Ramamurty, T.T. Goh, and Y. Li: Effect of crystallinity on the impact toughness of a La-based bulk metallic glass. *Acta Mater.* **48,** 2603 (2000).
130. J.J. Lewandowski: Effects of annealing and changes in stress state on fracture toughness of bulk metallic glass. *Mater. Trans., JIM* **42,** 633 (2001).
131. Z.F. Zhang, J. Eckert, and L. Schultz: Fracture mechanisms in bulk metallic glassy materials. *Phys. Rev. Lett.* **91,** 045505 (2003).

132. G. He, Z.F. Zhang, W. Löser, J. Eckert, and L. Schultz: Effect of Ta on glass formation, thermal stability and mechanical properties of a $Zr_{52.25}Cu_{28.5}Ni_{4.75}Al_{9.5}Ta_5$ bulk metallic glass. *Acta Mater.* **51,** 2383 (2003).
133. Y.F. Sun, S.K. Guan, B.C. Wei, Y.R. Wang, and C.H. Shek: Brittleness of Zr-based metallic glass matrix composites containing ductile dendritic phase. *Mater. Sci. Eng., A* **406,** 57 (2005).
134. M. Kusy, U. Kühn, A. Concustell, A. Gebert, J. Das, J. Eckert, L. Schultz, and M.D. Baro: Fracture surface morphology of compressed bulk metallic glass-matrix-composites and bulk metallic glass. *Intermetallics* **14,** 982 (2006).
135. Z.F. Zhang, J. Eckert, and L. Schultz: Difference in compressive and tensile fracture mechanisms of $Zr_{59}Cu_{20}Al_{10}Ni_8Ti_3$ bulk metallic glass. *Acta Mater.* **51,** 1167 (2003).
136. A.S. Argon and M. Salama: The mechanism of fracture in glassy materials capable of some inelastic deformation. *Mater. Sci. Eng.* **23,** 219 (1976).
137. G. He, W. Löser, J. Eckert, and L. Schultz: Phase transformation and mechanical properties of Zr-base bulk glass-forming alloys. *Mater. Sci. Eng., A* **352,** 179 (2003).
138. M.L. Falk and J.S. Langer: Dynamics of viscoplastic deformation of amorphous solids. *Phys. Rev. E* **57,** 7192 (1998).
139. A.S. Argon: Mechanism of inelastic deformation in metallic glass. *J. Phys. Chem. Solids* **43,** 945 (1982).
140. F. Spaepen: Microscopic mechanism for steady-state inhomogeneous flow in metallic glasses. *Acta Metall.* **25,** 407 (1977).
141. K. Hajlaoui, A.R. Yavari, B. Doisneau, A. LeMoulec, W.J.F. Botta, G. Vaughan, A.L. Greer, A. Inoue, W. Zhang, and A. Kvick: Shear delocalization and crack blunting of a metallic glass containing nanoparticles: In situ deformation in TEM analysis. *Scripta Mater.* **54,** 1829 (2006).
142. A. Inoue, W. Zhang, T. Tsurui, A.R. Yavari, and A.L. Greer: Unusual room-temperature compressive plasticity in nanocrystal-toughened bulk copper-zirconium glass. *Philos. Mag. Lett.* **85,** 221 (2005).
143. E. Pekarskaya, C.P. Kim, and W.L. Johnson: In situ transmission electron microscopy studies of shear bands in a bulk metallic glass based composite. *J. Mater. Res.* **16,** 2513 (2001).
144. K.B. Kim, J. Das, F. Baier, and J. Eckert: Propagation of shear bands in $Ti_{66.1}Cu_8Ni_{4.8}Sn_{7.2}Nb_{13.9}$ nanostructure-dendrite composite during deformation. *Appl. Phys. Lett.* **86,** 171909 (2005).
145. K.B. Kim, J. Das, F. Baier, and J. Eckert: Lattice distortion/disordering and local amorphization in the dendrites of a $Ti_{66.1}Cu_8Ni_{4.8}Sn_{7.2}Nb_{13.9}$ nanostructure-dendrite composite during intersection of shear bands. *Appl. Phys. Lett.* **86,** 201909 (2005).
146. J. Das, M.B. Tang, K.B. Kim, R. Theissmann, F. Baier, W.H. Wang, and J. Eckert: "Work-hardenable" ductile bulk metallic glass. *Phys. Rev. Lett.* **94,** 205501 (2005).
147. J. Schroers and W.L. Johnson: Ductile bulk metallic glass. *Phys. Rev. Lett.* **93,** 255506 (2004).
148. J. Saida, A.D.H. Setyawan, H. Kato, and A. Inoue: Nanoscale multistep shear band formation by deformation-induced nanocrystallization in Zr–Al–Ni–Pd bulk metallic glass. *Appl. Phys. Lett.* **87,** 151907 (2005).
149. D.S. Sung, O.J. Kwon, E. Fleury, K.B. Kim, J.C. Lee, D.H. Kim, and Y.C. Kim: Enhancement of the glass forming ability of Cu–Zr–Al alloys by Ag addition. *Metals Mater. Int.* **10,** 575 (2004).
150. M. Chen, A. Inoue, W. Zhang, and T. Sakurai: Extraordinary plasticity of ductile bulk metallic glasses. *Phys. Rev. Lett.* **96,** 245502 (2006).
151. K.B. Kim, J. Das, S. Venkataraman, S. Yi, and J. Eckert: Work hardening ability of ductile $Ti_{45}Cu_{40}Ni_{7.5}Zr_5Sn_{2.5}$ and $Cu_{47.5}Zr_{47.5}Al_5$ bulk metallic glasses. *Appl. Phys. Lett.* **89,** 071908 (2006).
152. J. Das, S. Pauly, C. Duhamel, B.C. Wei, and J. Eckert: Microstructure and mechanical properties of $Cu_{47.5}Zr_{47.5}Al_5$. *J. Mater. Res.* 22(2) 326, (2007).
153. J. Das, K.B. Kim, W. Xu, B.C. Wei, Z.F. Zhang, W.H. Wang, S. Yi, and J. Eckert: Ductile metallic glasses in supercooled martensitic alloys. *Mater. Trans., JIM* **47,** 2606 (2006).
154. Y.F. Sun, B.C. Wei, Y.R. Wang, W.H. Li, T.L. Cheung, and C.H. Shek: Plasticity improved Zr–Cu–Al bulk metallic glass matrix composites containing martensite phase. *Appl. Phys. Lett.* **87,** 051905 (2005).
155. Z.W. Zhu, H.F. Zhang, W.S. Sun, B.Z. Ding, and Z.Q. Hu: Processing of bulk metallic glass with high strength and large compressive plasticity in $Cu_{50}Zr_{50}$. *Scripta Mater.* **54,** 1145 (2006).
156. P. Jia, H. Guo, Y. Li, J. Xu, and E. Ma: A new Cu–Hf–Al ternary bulk metallic glass with high glass forming ability and ductility. *Scripta Mater.* **54,** 2165 (2006).
157. V.N. Novikov and A.P. Sokolov: Poisson's ratio and the fragility of glass-forming liquids. *Nature* **431,** 961 (2004).
158. C.A. Angell: Formation of glasses from liquids and biopolymers. *Science* **267,** 1924 (1995).
159. M.J. Demkowicz and A.S. Argon: High-density liquidlike component facilitates plastic flow in a model amorphous silicon system. *Phys. Rev. Lett.* **93,** 025505 (2004).
160. M.J. Demkowicz and A.S. Argon: Autocatalytic avalanches of unit inelastic shearing events are the mechanism of plastic deformation in amorphous silicon. *Phys. Rev. B* **72,** 245206 (2005).
161. Q.K. Li and M. Li: Molecular dynamics simulation of intrinsic and extrinsic mechanical properties of amorphous metal. *Intermetallics* **14,** 1005 (2006).